Electrochemical Characterization of Platinum based anode catalysts for Polymer Exchange Membrane Fuel Cell

By

Oko Unathi Gcilitshana

A thesis submitted in fulfilment of the requirements for the degree of Magister Scientiae in the Department of Chemistry, University of the Western Cape.

Supervisor: Dr. L. Khotseng

Co-supervisor: Dr. S. Pasupathi

December 2008

DECLARATION

I declare that “Electrochemical Characterization of Platinum based anode catalysts for Proton Exchange Membrane Fuel Cell” is my own work, that it has not been submitted for any degree or examination in any other university, and that all the sources I have used or quoted have been indicated and acknowledged by complete references.

Oko Unathi Gcilitshana December 2008

Signed:…….

ABSTRACT

Electrochemical Characterization of Platinum based anode catalysts for Polymer Exchange Membrane Fuel Cell

Oko Unathi Gcilitshana

M.Sc. Thesis, Department of Chemistry, University of the Western Cape

The present state-of-art Proton Exchange Membrane Fuel Cell (PEMFC) technology is based on platinum (Pt) as a catalyst for both the fuel (anode) and air (cathode) electrodes. Platinum is highly active but susceptible to poisoning by CO, which may be present in the H_2-fuel used, especially when it is generated through reforming. Presence of trace amount of CO in the H_2-fuel poisons the anode irreversibly and decreases the performance of the PEMFCs. Binary and ternary supported catalysts have been investigated for improving the performance of PEM fuel cells. Combining Pt with additional elements reduces the overpotential for reactions critical to the power density of PEM fuel cells. Supporting binary and ternary catalysts on carbon increases catalyst utilization, and allows high PEM fuel cell performance at low metal loading.

In this study, the main objective was to investigate the tolerance of platinum based binary anode catalysts for CO poisoning from 10ppm up to1000ppm and to identify the best anode catalysts for PEMFCs that tolerates the CO fed with reformed hydrogen.

Selected platinum based binary catalysts were screened for their activity, hydrogen oxidation and tolerance to CO. The amount of CO was varied between 10ppm and 1000ppm and the tolerance of binary catalysts was evaluated. Also, the effect of sintering on the activity of binary catalysts, particularly on the particle size, dispersion and extent of alloying was studied in order to identify the best CO tolerant anode electrocatalyst. Chronoamperometry was used to screen the electrochemical activity and stability of catalysts. Physical characterizations of the catalysts were carried out using SEM, EDS, TEM and XRD analysis.

Commercial Pt/C used as the baseline was the best electrocatalyst that favored the HOR and in its unsintered state it proved to be the most stable. The binary catalysts used in this study tolerated the CO poisoning better than Pt/C used as a baseline. PtSn/C was identified as the best electrocatalyst because it showed better tolerance towards the CO poisoning than all the studied electrocatalyst. Sintering induced changes in electrocatalyst properties such as a nanoparticle size, morphology, dispersion of the metal on the support, alloying degree, electrocatalytic activity and stability. The dispersion of the metal on the support and electrocatalytic properties of the electrocatalysts were improved. The surface morphology improved from amorphous to more ordered states. The results obtained from SEM EDS showed that the platinum binary electrocatalysts are stable nature because their elemental composition remained the same before and after sintering. XRD results confirmed the crystalline particle structure of Pt and that the electrocatalysts exhibited a face centered cubic-structure. The average particle sizes obtained from XRD and TEM for both sintered and

unsintered electrocatalysts were 3.1nm and 2.9nm Pt/C, 3.1nm and 2.8nm PtRu/C, 3.3nm and 3.1nm PtNi/C and 2.9nm and 3.0nm PtSn/C respectively.

ACKNOWLEDGEMENTS

Almighty God for the favor He has bestowed upon my life, for if it was not him I would not be where I am. For His continuing patience and grace over my life.

Greatest appreciation to my parents, Mr. M.Z. Gcilitshana and his lovely wife Mrs. V.L. Gcilitshana, for supporting and encouraging me into being the best that I can be. Not forgetting my brother Mzontsundu. Gcilitshana for his moral support.

Huge thanks to Dr. S. Pasupathi for being there for me through out the research. Your guidance, support and patience are what made this research a success.

Prof. V.M. Linkov, Dr. L. Khotseng, and the staff of the South African Institute for Advanced Materials Chemistry for giving me an opportunity to conduct the research.

Mr. Adrian (Electron Microscopy Unit, Department of Physics, University of the Western Cape) Scanning Electron Microscopy, Transmission Electron Microscopy.

Dr. R. Bucher (Materials Research Group, iThemba Labs) Proton-Induced X-ray Emission Spectroscopy.

Last but not least, a heartfelt appreciation to Miss Nosipiwo Andiswa Valisi for the support in times of need.

The financial assistance of the National Research foundation (NRF) towards this research is hereby acknowledged.

TABLE OF CONTENTS

LIST OF FIGURES

LIST OF TABLES

LIST OF ABBREVIATIONS

EDS	**Energy Dispersive Spectroscopy**
HOR	**Hydrogen Oxidation Reaction**
PEMFC	**Proton Exchange Membrane Fuel Cell**
SEM	**Scanning Electron Microscopy**
TEM	**Transmission Electron Microscopy**
XRD	**X-Ray diffraction**
CO	**Carbon monoxide**

STRUCTURE OF THESIS

Chapter 1: **Literature review:** ***Background to the fuel cell technology***:

The literature review focuses on the fundamental issues that hinder the commercialization of Fuel cells, giving particular emphasis on PEMFC anode electrocatalysts. The physico-chemical and electrocatalytic properties of nanomaterials and the general principles in the preparation of nanophase electrocatalysts are also reviewed.

Chapter 2: **Methodology:**

Outlines the methods employed in the study, emphasizing on the characterization techniques employed in the study.

Chapter3: **Results and Discussion:** ***Structural Characterization of nanophase***

The results of the study are presented and discussed to provide insight into the effect of sintering conditions on the morphology of platinum based binary catalysts and their implications for their activity and CO tolerance.

Chapter4: **Results and Discussion:** ***Electrochemical Characterization of Electrocatalysts***

The results of the electrochemical characterization are presented and discussed. Half-cell studies were carried out to study the hydrogen oxidation activity and CO tolerance of platinum based catalysts in order to identify the best catalysts for PEMFC anode applications.

Chapter 5: **Conclusions and Recommendations**

CHAPTER 1

LITERATURE REVIEW

INTRODUCTION: MOTIVATION AND OBJECTIVES OF THE STUDY

1.1 BACKGROUND TO FUEL CELL TECHNOLOGY

Energy is the very lifeblood of today's society and economy. Our work, leisure, and our economic, social and physical welfare all depend on the sufficient, uninterrupted supply of energy. Traditional generation of energy such as combustion of fossil fuels oil, coal and gas which are ultimately limited and the growing gap between increasing demand and shrinking supply will, in the not too distant future, have to be met increasingly from alternative primary energy sources. The technologies employed, despite their advanced development, are inefficient and dirty, (generating significant proportion of our acid rain and greenhouse emissions). Though being inadequate, these technologies are continued to be used for the simple reason that no alternative can match them on cost or scale terms and meeting our energy needs, without causing the collapse of the ecosystems upon which we depend, has become a major concern to the governments, industry and individuals alike. This concern has brought about the development of a range of 'alternative' clean, renewable energy technologies such as solar photovoltaic and wind energy. However, these alone will not be enough due to their inherently variable output, the remoteness of prime locations, and the difficulty in efficiently and cost effectively storing and transporting energy. What is needed is a technology or combination of technologies which allow for the clean cost effective supply of energy on demand on a large scale and in any location.

There is one emerging and promising technology which could allow this demand to be met. This technology is the fuel cell, an electrochemical device that converts hydrogen and oxygen into electricity without combustion. When Christian Friedrich Schönbein

discovered the principle of a fuel cell in 1838 [1], little did he know that his discovery would be the proposed energy crisis breakthrough for the entire world in the 21st century. The first fuel cell was developed by Welsh scientist Sir William Robert Grove in 1843[1].

Basically there are five types of Fuel cells which are categorised by the type of the electrolyte employed. The electrolyte may consist of a liquid solution or a solid membrane material. DMFCs differ from the other types of fuel cells in that hydrogen is obtained from the liquid methanol, eliminating the need for a fuel reformer. A second grouping can be done by looking at the operating temperature for each of the fuel cells. There are, thus, low-temperature and high-temperature fuel cells. Low-temperature fuel cells are the Alkaline Fuel Cell (AFC), the Polymer Electrolyte Fuel Cell (PEMFC), the Direct Methanol Fuel Cell (DMFC) and the Phosphoric Acid Fuel Cell (PAFC). The high-temperature fuel cells operate at temperatures approx. 600±1000 ºC and two different types have been developed, the Molten Carbonate Fuel Cell (MCFC) and the Solid Oxide Fuel Cell (SOFC). An overview of the fuel cell types and characteristics is given in Table 1.1 below.

Table 1.1 Fuel Cell Types and Characteristics from Rocky Mountain Institute [2]

Fuel Cell Type	Electrolyte	Anode Gas	Cathode Gas	Temperature	Efficiency
Proton Exchange Membrane (PEM)	solid polymer membrane	hydrogen	pure or atmospheric oxygen	75°C (180°F)	35–60%
Alkaline (AFC)	potassium hydroxide	hydrogen	pure oxygen	below 80°C	50–70%
Direct Methanol (DMFC)	solid polymer membrane	methanol solution in water	atmospheric oxygen	75°C (180°F)	35–40%
Phosphoric Acid (PAFC)	Phosphorous	hydrogen	atmospheric oxygen	210°C (400°F)	35–50%
Molten Carbonate (MCFC)	Alkali-Carbonates	hydrogen, methane	atmospheric oxygen	650°C (1200°F)	40–55%
Solid Oxide (SOFC)	Ceramic Oxide	hydrogen, methane	atmospheric oxygen	800–1000°C (1500–1800°F)	45–60%

1.1.1. Hydrogen Economy

Hydrogen is a fascinating energy carrier that can be produced from electricity and water. Its conversion to heat or power is simple and clean when combusted with oxygen, hydrogen forms water and no pollutants are generated or emitted (meaning less acid rain and greenhouse emissions). The water is returned to nature where it originally came from. But hydrogen, the most common chemical element in universe does not exist in nature in its pure form, it has to be separated from chemical compounds, by electrolysis from water or by chemical processes from hydrocarbons or other hydrogen carriers. The electricity for the electrolysis may eventually come from clean renewable sources such as solar radiation, kinetic energy of wind and water or geothermal heat. Therefore, hydrogen may become an important link between renewable physical energy and chemical energy carriers.

One of the main offerings of a hydrogen economy is that fuel cells can replace internal combustion engines and turbines as the primary way to convert chemical energy into kinetic or electrical energy. The reason to expect this changeover is that fuel cells, being electrochemical, are usually (and theoretically) more efficient than heat engines. Currently, fuel cells are more expensive to produce than common internal combustion engines, but are becoming cheaper as new technologies and production systems develop.

1.2 RATIONALE TO THE RESEARCH

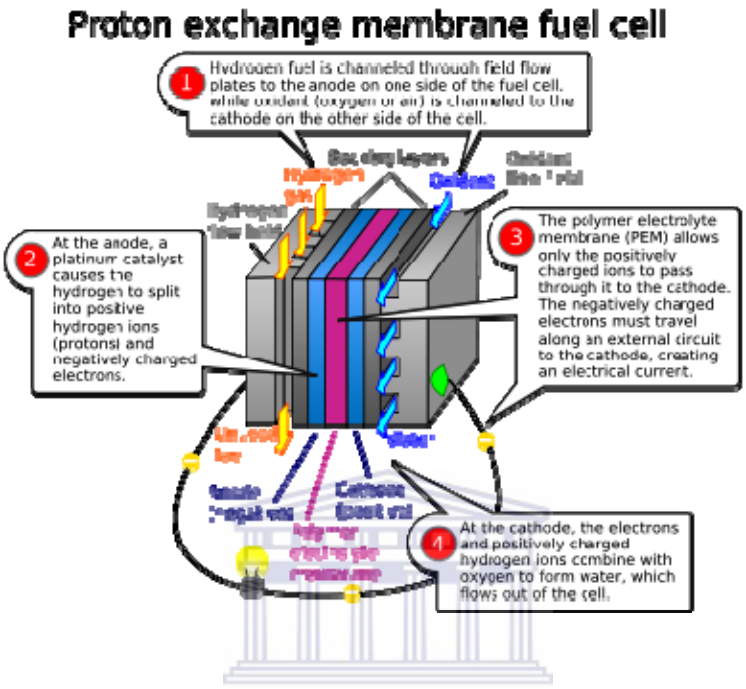

Figure 1.1: Diagram of a PEMFC [3]

This research focuses on one of the low temperature fuel cells, the Proton Exchange Membrane Fuel Cell (PEMFC). PEMFCs are highly efficient power generators, achieving up to 50-60% conversion efficiency, even at sizes of a few kilowatts. They have zero pollutant emissions when fuelled directly with hydrogen, unlike DMFC which emits CO_2, and near zero emissions when coupled to reformers. They also minimise the use of fossil fuels contributing to lowering of environmental pollution. These attributes make them potentially attractive for a variety of applications including electric vehicles and distributed generation and cogeneration of heat and power in buildings. Over the past few years, there have been intense efforts worldwide to develop low-cost PEMFC systems with the primary

focus being on vehicle applications, but now there is an equally important application which is combined heat and power generation in commercial and residential buildings.

PEMFCs produce electricity from external supplies of fuel (on the anode side) and oxidant (on the cathode side). These react in the presence of an electrolyte which plays a vital role in the functioning of the fuel cell as it acts as a separator for the fuel and oxidant and permits only the appropriate ions to pass between the anode and cathode. The electrolyte must be hydrated sufficiently to facilitate the transfer of ions. If water is evaporated too quickly, the membrane dries, resistance across it increases and eventually it will crack, creating a gas "short circuit" where the hydrogen and oxygen combine directly, thereby damaging the fuel cell. If the water is evaporated too slowly, the electrodes will flood, preventing the reactants from reaching the catalyst and stopping the reaction.

Hydrogen molecules (fuel) enter a fuel cell at the anode where a chemical reaction strips them of their electrons. The hydrogen molecules are now "ionized," and carry a positive charge, which then travels through the membrane to the cathode. The negatively charged electrons provide the current through external circuit to do work. Oxygen (oxidant) enters the fuel cell at the cathode and it there combines with electrons returning from the external circuit and hydrogen ions that have travelled through the electrolyte to form water, which drains from the cell. As long as a fuel cell is supplied with hydrogen and oxygen, it will generate electricity. Even better, since fuel cells create electricity chemically, rather than by combustion, they are not subject to the thermodynamic laws that limit a conventional power plant.

The PEMFCs are currently not available to the average consumer. This hydrogen fuel cell still has obstacles to overcome before it can become commercially feasible. For instance, the most efficient fuel for use in a PEMFC is pure hydrogen which has a high production cost and no existing infrastructure to store. Reforming from hydrocarbons, including

gasoline and alcohol is the most extensively used technique for generating hydrogen fuel for use in PEMFCs, which contain 45% hydrogen, 10-1000ppm CO, 15% CO_2 and 1% CH_4.

The electrochemical reactions in a fuel cell consist of two separate reactions: an oxidation reaction at the anode and a reduction reaction at the cathode. Normally, the two reactions would occur very slowly at the low operating temperature of the PEM fuel cell. So, catalysts are used to speed up the reaction of oxygen and hydrogen. Platinum is the best single metal catalyst known yet for PEMFC applications. The catalyst is supported on high surface area carbon, so that the maximum surface area of the platinum can be exposed to the hydrogen or oxygen.

Under normal circumstances, hydrogen gas enters the anode of the fuel cell and electrooxidizes on the platinum catalyst in two steps. The first step is when hydrogen dissociates requiring two free adjacent platinum sites.

$$H_2 + 2\,(Pt) \leftrightarrow 2(Pt\text{-}H) \qquad [1]$$

The second step involves the dissociation of hydrogen into two hydrogen ions (protons) and two electrons:

$$2(Pt\text{-}H) \leftrightarrow \quad 2(Pt) + 2H^+ + 2e^- \qquad [2]$$

When a CO-contaminated hydrogen gas stream enters the anode, the CO can adsorb onto either a bare platinum site or a platinum-hydrogen site.

$$CO + (Pt) \rightarrow (Pt{=}\,CO) \qquad [3]$$

$$2CO + 2(Pt\text{-}H) \rightarrow 2(Pt{=}\,CO) + H_2 \qquad [4]$$

The adsorbed CO blocks active platinum sites at the anode, as shown in the representation in Figure **2,** leading to the inhibition of reactions [l] and [2] and to performance losses.

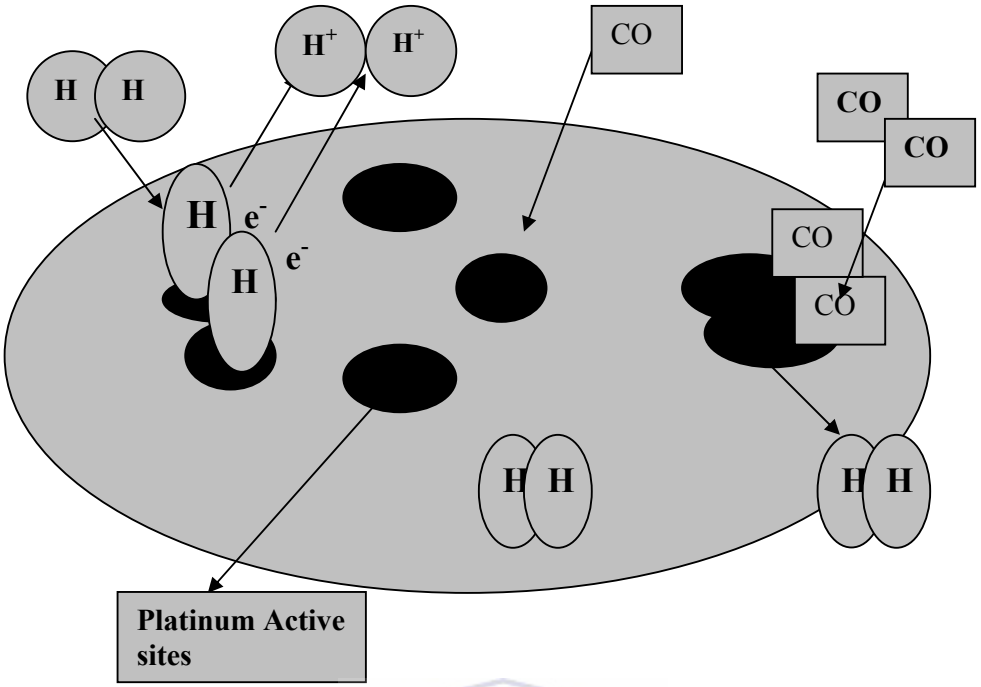

Platinum Catalyst Surface

Figure 1.2. A schematic of the CO adsorption theory on the platinum catalyst

1.3 FUNDAMENTALS OF ELECTROCATALYSTS

1.3.1 Overview of electrocatalysts

The phrase *catalysis* was originated by Jöns Jakob Berzelius who in 1835 was the first to note that certain chemicals speed up a reaction. Catalysis is a way of accelerating the rate of a chemical reaction by means of contacting the reactants with a substance called a catalyst, which itself is not consumed by the overall reaction. It does so by providing an alternative route to products and this alternative route being subject to lower activation energy than in the uncatalyzed reaction and this lowered activation energy increases the reaction rate. As observed in Figure 1.3, the activation energy of a catalyzed reaction is distinctively lower than that of an uncatalyzed reaction .The presence of the catalyst opens a different reaction pathway (shown in red) with lower activation energy and the final result and the overall thermodynamics are the same.

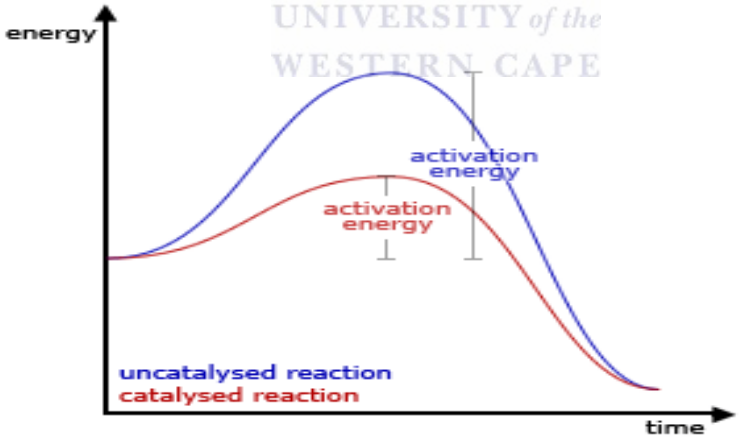

Figure 1.3. *Generic potential energy diagram showing the effect of a catalyst in a hypothetical exothermic chemical reaction.*

Catalysts can be either heterogeneous or homogeneous. Heterogeneous catalysts are present in different phases from the reactants (e.g. a solid catalyst in a liquid reaction mixture), whereas homogeneous catalysts are in the same phase (e.g. a dissolved catalyst in a liquid reaction mixture.

***Heterogeneous Catalysis*:** is a model of catalysis whereby a catalyst provides a surface on which the reactants become temporarily adsorbed. Bonds in the substrate become sufficiently weakened for new bonds to be created and these bonds between the products and the catalyst are weaker, so the products are released [4].

***Homogeneous Catalysis*:** in homogeneous catalysis the catalyst is a molecule which facilitates the reaction. The catalyst initiates reaction with one or more reactants to form intermediate(s) and in some cases one or more products. Subsequent steps lead to the formation of remaining products and to the regeneration of the catalyst [5].

***Electrocatalysis*:** is defined in its widest sense as the study of how reactions may be accelerated at electrodes. This often requires the surface of the electrode to be modified in some way or other for there to be a mediating molecule close to the electrode or in solution.

***Platinum Group Catalysts*:** because of their high chemical activity, they are better candidates for making hydrogen fuel cells more efficient.

Support Materials: It is well accepted that the surface properties of the carriers have a significant influence on the properties of the supported catalytically active species and there is also significant evidence that the nature of carbon carrier and the catalyst preparation protocol are key factors influencing the catalytic activity.

1.3.2 Preparation methods of electrocatalysts

Catalytic activity is closely dependent on the method of preparation. The determining factor between the techniques, for the selection of a suitable preparation method, is that most of the methods produce nanophase electrocatalysts with different particle size distributions; average particle sizes; and particle dispersions in the case of supported catalysts. For the preparation of Pt based electrocatalysts five general methods have been employed [6]:

i) Impregnation-reduction method

ii) Pt precursors and precipitation method

iii) Sulphite method

iv) Bönnemann method

v) Adams method

1.4.2.1 Impregnation

The simplest method for preparation of supported catalysts is impregnation. In this method, a solution of metal salt(s) is prepared and mixed with the carbon support. The resulting slurry is dried to remove the solvent and the material is usually heat-treated and/or reduced to decompose the salt to give the desired form of the catalyst. The advantages of the impregnation-reduction method are the simplicity of the method and its applicability to the preparation of a large number of supported nanophase electrocatalysts. Advantageously, the metal loading can be controlled by varying the quantity of the metal salt precursor added to the colloidal solution. However, impregnation is not favoured as a large-scale preparation method due to difficulties associated with dry mixing of carbon black and the poor wetting of carbons by aqueous solutions [7]. A variation of this method is incipient-wetness impregnation.

1.3.2.2 Precipitation

The majority of methods used for the preparation of Pt-based catalysts are based on precipitation. These are generally based on the precipitation of a soluble species by chemical transformation. This can be in the form of a change in pH (e.g. from acidic to basic) or the addition of a reducing agent (e.g. formaldehyde to precipitate metal) [7]

1.3.2.3 Sulphite method

The sulphite method is based on sulphito chemistry and involves formation of sulphito complexes of the general form $[H_xPt(SO_3)_4]^{-(6-X)}$ in solution. These complexes are then oxidized where the sulphito-ligands are converted to sulphate which does not coordinate under the conditions used. This leaves on unstable $[Pt(OH)_n]^{-(n-2)}$ species that aggregates to form small colloidal particles (2nm).

The advantage of the method is that even at high loadings, the particles show little tendency to aggregate, but the pH must be very carefully controlled, which is essential if uniform 2nm particles are to be obtained [8].

1.3.2.4 Bönnemann Method

Bönnemann method [9] is based on surfactant shell stabilizing Pt colloid particles in an organic solvent whereby a solution of the reducing agent, $Al(CH_3)_3$, is mixed with a solution of the metal salt, $Pt(acac)_2$ and kept at 60°C for 16 hours to optimize the reduction reaction. Colloids are then supported on a high-surface-area carbon by adding the colloid dispersion in toluene. Finally, the solvent is evaporated and the catalyst rinsed with pentane [10]. In particular, this method has been used to prepare bi-metallic catalysts with narrow particle size distributions and alloy structures [11].

1.3.2.5 Adams method

As well as carbon-supported Pt-based catalysts, metal blacks (unsupported metal powders) are used in certain applications where the loading of metal in electrodes is not critical (e.g. DMFCs). This method is the classic method for preparing unsupported porous metal powders [12].

Normally, metal for metal blacks can be prepared in a manner similar to supported metal catalysts using the precipitation method described above. In addition, metal blacks can be prepared by direct reduction of metal salt solutions with a reducing agent. However, this method is not used extensively for preparing metal blacks for fuel cell use due to the difficulty in removing impurities [13].

1.3.3 Support Materials

The choice of an electrode material is not an easy task as the criteria it should satisfy are very strict. Electrode materials should be (a) catalytically active, (b) chemically and mechanically stable and (c) inexpensive. Pt satisfies the former two but high cost limits its commercial application. Non platinum active metals which are considerably cheap, exist, however these suffer of corrosion, passivity and similar difficulties. One of the important tasks of electrocatalysis is to reduce or replace Pt completely. Two approaches to obtain cheaper and active catalysts (a) to develop multicomponent catalysts with the activity similar or higher than that of Pt. (b) increase the surface area by lowering the particle size to nano scale as well as reducing the catalyst loading on the electrodes. During recent years, carbon blacks such as Vulcan XC-72 have received increasing attention for applications as a support material in fuel cell electrodes.

1.3.3.1 Carbon Black

Carbon black is a generic term for a particulate form of elemental carbon manufactured by thermal decomposition, including detonation, or by incomplete combustion of hydrocarbon compounds and has a well-defined morphology with a minimum content of tars or other extraneous materials. They are categorized, on the basis of different production processes by which they are made, as acetylene black, channel black, furnace black, lampblack or thermal black. It is used as a catalyst support in fuel cells because of its high electrical conductivity, good corrosion resistance, low cost compared with other supports such as alumina or silica, superior mechanical, thermal and chemical stability, ability to modify the chemical nature of the surface, control porosity and ability to recover the supported catalyst by burning away the carbon support etc. The loading of platinum on carbon can vary from 10% to 90% of platinum on carbon.

Carbon black is composed of particles (ranging from 10 to 100nm) that are fused together to form aggregates with high developed surface area of 250 $m^2 \cdot g^{-1}$ [14].Several aggregates interact through Van der Waals forces to give place to a secondary structure known as agglomerate. Contrary to the aggregates, agglomerates are broken under mechanical stress into smaller units. Fig 2. 2(a) shows a scheme of a CB aggregate while in Fig. 2. 2(b) an aggregate TEM picture can be observed.

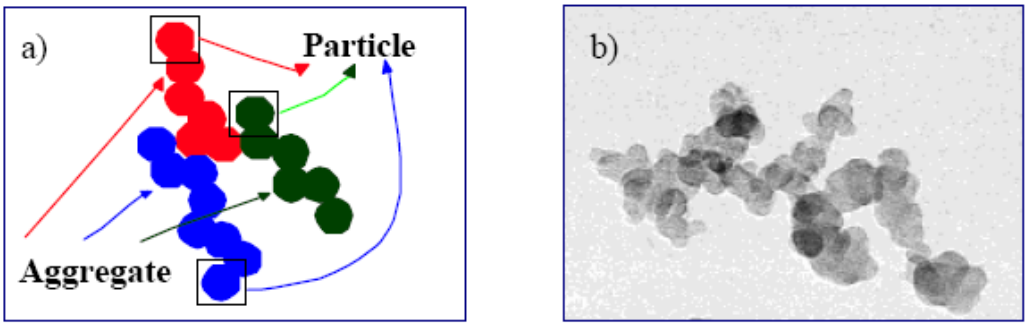

Fig. 1.4 (a) *CB agglomerate scheme b) image of an agglomerate from Sid Richardson Carbon Black Co.*

There is, however, a number of problems, which complicates interpretation of the results obtained using commercial catalysts. These are poisoning of metal by the impurities present in technical carbon materials (in particular sulfur), rather wide particle size distributions, metal agglomeration, etc. For example, agglomeration may not only result in a decrease of the metal utilization, but also in drastic changes in reactivity due to the formation of particular nanostructures with high concentration of grain boundaries.

1.3.3.2 Nanomaterials

Nanomaterials have ultra fine particles with a dynamic diameter of < 100 nm. They present several different morphologies (flakes, spheres, dendritic shapes, etc.) and are generally designed and manufactured with physical properties tailored to meet the needs of the specific application they are going to be used for. Nanomaterials have been described as *'novel materials whose size of elemental structure has been engineered at the nanometer scale'*. Over the past few decades, interest in the unique properties associated with materials having structures on a nanometer scale has been increasing at a high rate. This is mainly due to the nanometer size of the materials which render them: (i) large fraction of surface atoms; (ii) high surface energy; (iii) spatial confinement; (iv) reduced imperfections, which do not exist in the corresponding bulk materials [11].

For instance, a relatively inert metal or metal oxide may become a highly effective catalyst when manufactured as nanoparticles. Nanoparticles can consist of a range of different morphologies including nanotubes, nanowires, nanofibres and a range of spherical or aggregated dendritic forms. These materials have seen application in a wide range of industries including electronics, pharmaceuticals, chemical-mechanical polishing, catalysis, and it is likely that the next few years will see a dramatic increase in the industrial generation and use of nanoparticles.

1.3.3.2.1 Mechanical Properties of Nanomaterials

Due to the nanometer size, many of the mechanical properties of the nanomaterials are different from the bulk materials including the hardness, elastic modulus, fracture toughness, scratch resistance and fatigue strength etc. An enhancement of mechanical properties of nanomaterials can result due to this modification, which is generally a resultant from structural perfection of the materials. The small size either renders them free of internal structural imperfections such as dislocations, micro twins, and impurity precipitates or the few defects or impurities present can not multiply sufficiently to cause mechanical failure. Also the imperfections within the nano dimension are highly energetic and will migrate to the surface to relax themselves under a process of heat treatment where they purify the material, leaving perfect material structures inside the nanomaterials. Moreover, the external surfaces of nanomaterials also have less or are free of defects compared to bulk materials, serving to enhance the mechanical properties of nanomaterials. One of the nanomaterials that have been found to have excellent mechanical properties are carbon nanotubes which are principally used as catalyst support and H_2 storage materials. Since their discovery, carbon nanotubes as the smallest carbon fibers discovered have stimulated intensive research interests. The unique properties of nanomaterials present an opportunity to use them in novel applications and devices.These enhanced mechanical properties of the nanomaterials could have many potential applications both in nano scale such as mechanical nano resonators, mass sensors, microscope probe tips and nano tweezers for nano scale object manipulation. Among many of the novel mechanical properties of nanomaterials, high hardness has been discovered from many nanomaterials system. [15-18]

1.3.3.2.2 Electrocatalytic Properties of Nanomaterials

Nanomaterials have emerged as intriguing materials for diverse applications that include catalysis [18] due to their specific structures, interesting properties that differ from their solid counterparts. Nanomaterials based catalysts are usually heterogeneous catalysts and when they are used in electrocatalytic applications they are termed *"nanophase electrocatalysts"*.Their extremely small size maximizes the surface area exposed to the reactants allowing more reactions to occur. Therefore if the electrocatalytic activity increases as the surface area increases, nanomaterials are the best candidates as they possess high surface area.

For numerous nanocatalysts, Pt and Pt-based nanomaterials are still indispensable and are the most effective catalysts and numerous literatures have been reported to design unsupported or supported Pt catalyst [19], however, a critical problem with Pt-based catalysts is their prohibitive cost. Hence many efforts have focused on the development of a novel approach to produce hollow Pt catalysts with a high-surface area to achieve high-catalytic performance and utilization efficiency or replace it with less expensive materials [20].

1.3.4 Metal-Support Interactions

Recognizing the ever-present and critical role of catalysis in fuel cell technology, the role of metal-support interaction on stability and reactivity of novel catalysts is being exploited. The interaction between the active component and the support is of great importance for the catalytic behavior of a heterogeneous catalyst. Thus the activity and selectivity of a supported metal catalyst may be altered by changing the nature of the support. Catalyst stability and resistance against sintering are also dependent on metal-support interactions. The specific catalysts examined consist of metal nanoparticles anchored to carbon and

oxide supports. The former is used for electrodes (membrane or traditional carbon mesh) and the latter for fuel processing catalysts.

1.4. SINTERING EFFECT ON ELECTROCATALYSTS

At the current technical stage, the most practical catalysts in fuel cells are highly dispersed platinum (Pt)-based nanoparticles. However, there are several drawbacks to Pt based catalysts, such as high cost, sensitivity to contaminants, relatively low tolerance to CO poisoning. With respect to the exploration of alternative non-Pt catalysts, several other types of catalysts, including supported platinum group metal (PGM) such as Pd-, Ru-and Ir-based catalysts, bimetallic alloy catalysts, transition metal macrocycles, and transition metal chalcogenides, have been employed for PEM fuel cell catalysis [21-23]. The major force driving the development of non-Pt catalysts is a reduction in cost. However, these approaches are still in the research stage, as catalyst activity and stability are still too low to be practical when compared to Pt-based catalysts. It is well known that the electrocatalyst performance is strongly dependent on the preparation procedures, including the addition of metal and its precursor, the support type and supporting strategy, and the heat-treatment strategy [24–30]. For example, even if the same catalyst with the same catalyst loading is used, the catalytic activity will differ depending on how the catalysts were attached to the electrode surfaces

Regarding Pt-based catalyst synthesis, Wang et al. [23-27, 31] mentioned that heat-treatment has been recognized as an important and sometimes necessary step for catalytic activity improvement. Its benefits being to remove any undesirable impurities resulting from early preparation stages, to allow a uniform dispersion and stable distribution (*from amorphous to more ordered states*) of the metal on the support, and, therefore, to improve the electrocatalytic activity of the synthesized catalyst [24].

Many heat-treatment techniques, such as traditional oven/furnace heating [27, 32], have been applied to prepare PEM fuel cell electrocatalysts. Among these, the traditional oven/furnace heating technique is the most widely used. In general, it involves heating the catalyst under an inert (N_2, Ar, or He) or reducing (H_2) atmosphere in the temperature range of 80–900°C for 1–4 hours [24, 27] For example, heat treatment or thermal activation for Pt based catalyst synthesis has been considered a necessary step, which has a significant impact on the metal particle size and size distribution, particle surface morphology, and metal dispersion on the support [28].

1.5 BINARY ELECTROCATALYSTS

At present, pure platinum is the most commonly used electrocatalyst materials for PEMFC. Though platinum shows the best activity in PEMFC when pure H_2 is used as anode fuel, the presence of CO in the H_2 gas stream, even at low ppm levels poisons the catalyst irreversibly thereby affecting its catalytic activity and stability.

In an attempt to reduce the degree of catalytic deactivation of the catalyst and to reduce catalyst cost second metals were applied to make alloys with Pt; a mechanical alloying technique was employed to refine the catalyst microstructure (i.e. increasing the effective catalyst surface area) [33-38]. Alloyed catalysts receive considerable attention, because of their unique catalytic properties; they often show higher selectivity, activity, and stability compared to the pure metal particles

For a Pt–M/C catalyst, the catalytic activity as well as the stability depends not only on the nature of Pt, but also on the second metal.

1.5.1 Structural Effects of Electrocatalysts

1.5.1.1 Effects of electrocatalyst particle size on electrochemical activity

It is reported that a particle size and distribution of Pt-based catalysts are key factors that determine their electrochemical activity and cell performance for fuel cells. But according to Coloma et al. [30]; the optimum catalyst size for a given electrochemical reaction cannot be predicted. Through reducing catalyst sizes into the nanoscale region, many research groups have observed structure-sensitive behaviour of the electrocatalysts in which the electrocatalytic activity begins to deviate from that of the bulk at a critical nanoparticle catalyst size [30, 31]. To account for this deviation in electrocatalytic activity, or particle size effect, many different theories have been proposed.

Taylor proposed that for a reaction to occur on a catalyst surface, it requires a specific number of catalyst atoms [32]. Working with this theory, [33-35] postulated that as a catalyst particle is decreased in size, there is a change in the ratio of catalyst sites. These sites have been characterized both in terms of their location on the catalyst particle and relative to other catalyst atoms (edge/corner locations and crystallographic planes). If the ratio of the catalyst sites were to change with respect to particle size, it would cause a change in the electrocatalytic activity.

1.5.1.2 Effects of particle surface morphology on electrochemical activity

It is known that not only the size of platinum particles but also increasing surface roughness of the catalyst plays an important role in the hydrogen oxidation kinetics for fuel cell applications in terms of both electrocatalytic activity and practical application of catalysts. There are more fractures on vertices, edge and corner sites of Pt particles with increasing surface roughness. As the fractures increase, the electrocatalytic activity increases with respect to the number of Pt atom located at vertices, edges and corners.

According to the investigation of Y. Morimoto et al. [39], of the electrochemical characteristics of Pt electrodes, the CO_{ad} oxidation characteristics on rough Pt electrode surfaces are much better than the smooth ones. H. Hoster et al. [40] also came to a similar conclusion. They compared the different electrochemical activities of smooth PtRu and multi-pore rough PtRu catalysts and found that the rough PtRu catalyst does have higher electrocatalytic activity than the smooth one.

1.6 OBJECTIVES OF THE STUDY

The main objective of this dissertation is to investigate the tolerance of platinum based binary anode catalysts for CO from 10ppm up to1000ppm in order to identify the best anode catalysts for PEMFCs, operating with reformed hydrogen.

A detailed literature survey helped us to identify CO tolerant platinum based binary catalysts as PtRu/C, PtNi/C and PtSn/C. The CO tolerance and HOR activity of the catalysts will be evaluated under various concentrations of CO, ranging from 0 to 1000ppm and will be compared to that of Pt/C in order to determine the poisoning effects of CO and to identify the best CO tolerant catalyst.

In our quest to identify the best CO tolerant HOR catalysts, the work will address the following fundamental issues of PEMFC anode catalysts:

- the effect of sintering on the morphology of the catalysts and its relation to the CO tolerance and catalytic activity.
- the effect of extent of alloying related to the CO tolerance and activity of the catalysts.
- the electrochemical characterizations such as cyclic voltammetry and chronoamperometry and physical characterizations such as SEM, TEM, EDS and XRD analysis will be done.

CHAPTER 2

METHODOLOGY

The characterization of nanophase electrocatalysts is the rational step after their preparation and prior to their application. The characterization of physical and chemical properties forms the starting point of the optimization in order to achieve the future possibility of cost-reduction and high electrocatalytic performance of nanophase catalysts. Various techniques are used as will be further specified.

2.1 MATERIALS AND METHODS

2.1.1 Materials

The commercial catalysts used in the study were Pt/C, PtRu/C, PtSn/C and PtNi/C purchased from BASF and the materials employed to prepare the various Anode Electrode Assemblies are shown in Table 2.1.

Table 2.1: Materials for preparing Anode electrode assembly

Type	Source	Specifications
Nafion®	Ion power, Inc	Liquion-11005wt%
Iso-2-propanol	Kimix	99.9%
Ultra-pure water	SAIAMC	Zeneer Power Purification System
Carbon paper	BASF	Toray Carbon paper 30%Teflon treated, Thickness 100μm
Nafion® membrane	Electrochem Inc.	1135
Spray Gun	Electrochem Inc	N_2 pressure

2.1.2 Heat Treatment of catalyst

The quartz tube in a tube furnace was pre-purged with dry nitrogen gas flowing at 500 ml/min for 45 min to suppress possible surface oxidation of Pt particles due to the remaining oxygen within the tube during the heat treatment. After pre purging the quartz tube the tube furnace was then pre heated to a target temperature of 350°C and 450°C. After the desired temperature was reached, an alumina boat loaded with the electrocatalyst was inserted into the center of a quartz tube. The samples were heated at the target temperatures for 3 hours under nitrogen gas flowing simultaneously at a rate of 5 ml/min. When the heating time was over, the tube was cooled down with the nitrogen gas still constantly flowing at 5ml/min.Then after the tube had cooled down the catalysts were taken out and grinded using a pestle and a mortar for 5 minutes.

2.1.3 Electrode Ink preparation

A schematic of the electrode preparation is provided below.

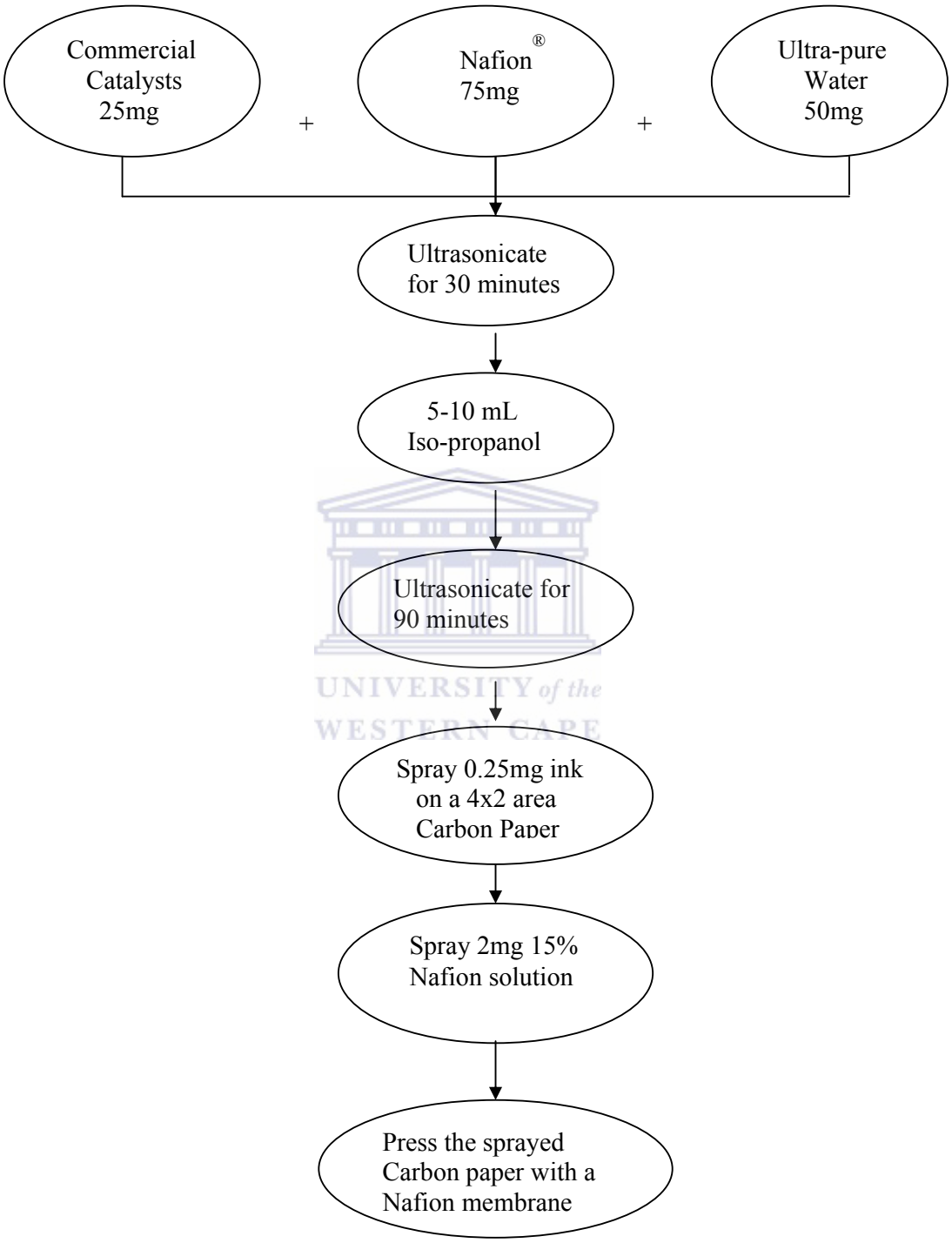

Figure 2.1 Process scheme for electrode preparation.

2.1.4 Treatment of the Nafion® membrane

- Boil 9 M HNO_3 in a 600mL Beaker (385mL HNO_3 +115mL Ultra pure water)
- Add membranes and boil for an hour
- Wash thoroughly with UP water ~ 500mL (3-4 times)
- Again boil 9M HNO_3
- Add membranes and boil for an hour
- Wash thoroughly with UP water ~ 500mL (5-6 times)
- Treat the membranes with H_2O_2 (5-10%) in a 600mL Beaker for an hour
- Boil 1M H_2SO_4 (27mL H_2SO_4 + 473mL UP water)
- Add membranes and boil for an hour
- Wash thoroughly with UP water ~ 500mL (5-6 times)
- Store in a beaker with UP water covered with a Para film

HNO_3 – Removes impurities

H_2O_2 – Oxidizes organic impurities.

H_2SO_4 – Protonates the membrane

2.1.4 Preparation of an Anode Electrode Assembly

The membrane treated in Section 2.1.4 is then pressed onto a Gas diffusion electrode using a hot presser at 130 ºC for 5minutes at 600bar.

2.2 PHYSICO-CHEMICAL CHARACTERIZATION OF ELECTROCATALYST

A whole range of physical characterization techniques can be applied to the study of fuel cell catalysts and several techniques are described in the literature. Since this study focuses on the experimental determination of the CO tolerance and HOR activity of t he catalysts, it focuses on specific characterization techniques that provides support information to the electrochemical characterizations such as

- X-ray Diffraction (XRD)
- Transmission Electron Microscopy (TEM)
- Scanning Electron Microscopy (SEM)
- Energy Dispersive Spectroscopy (EDS)

2.2.1 X-Ray Diffractometry

X-ray diffractometry (XRD) is a powerful tool in the study of crystallinity and atomic structure of materials and forms an integral part in a comprehensive characterization study of nanophase electrocatalysts. It is one of the most important non-destructive tools to analyze all kinds of matter, ranging from thin films and fluids to powder and crystals. XRD is an indispensable method for material characterization. For the purpose of this study XRD was used in the investigation of the crystalline structure, particle size and lattice parameters.

In the XRD analysis, the samples were mounted on a glass sample holder and the surface was flattened to allow maximum x-ray exposure.

The specifications of the Siemens D8 Advance XRD unit and operation parameters are tabled in Table 2.3.

Table 2.3: The Bruker AXS D8 Advance operational parameters.

Parameter	***Conditions***
X-ray detector	Lynx-Eye position sensitive detector
Tube	Copper K-alpha
Monochromator	None
Scanning range (2θ)	(25-90)º
Generator operation	40 kV and 40 mA
Current	40mA
X-ray source	Cu Kα (& = 1.5418 Å)

Crystallite size determination is performed by measuring the broadening of a particular peak in a diffraction pattern associated with a particular planar reflection from within the crystal unit cell. Particle size is inversely related to the half-width at half maximum of an individual peak. Typically, the narrower and more intense the peak, the larger the crystallite size. This is due to the periodicity of the individual crystallite domains, in phase, reinforcing the diffraction of the X-ray beam, resulting in a tall narrow peak [41]. The breadth of the diffraction peak is related to the size of the crystals by the Scherrer equation as given below:

$$D = 0.9\,\lambda / (B \cos\theta_{max}) \qquad [2\text{-}1]$$

Where, D = particle size (nm)

0.9 = shape factor

λ = x-ray wavelength (nm)

θ = angle of reflection (2θ)

B = peak-width at half peak-height (radians) [42]

Furthermore, the lattice parameter (α) can be calculated by the following equation:

$$a_0 = d\,[(h2 + k2 + l2)]^{1/2} \qquad [2\text{-}2]$$

Where h, k, and l constitute the Miller indices of a crystal facet, and d is the interplanar spacing determined using Braggs' Law.

$$n\lambda = 2d\sin\theta \qquad [2\text{-}3]$$

2.2.2 Transmission Electron Microscopy (TEM)

In this study, TEM was utilized in the direct examination of metal nanoparticle size; particle distribution; homogeneity of dispersion; and agglomeration of the metal phase in supported nanophase electrocatalysts.

In TEM operation, a narrow electron beam originating from a tungsten filament is concentrated onto ultra-thin sample surfaces using a series of magnetic lenses. The electrons interact with sample atoms while penetrating the thin sample structure leading to the transmittance of electrons and the production of secondary electrons. Secondary electrons pass through an aperture to produce an image on a fluorescent screen. For carbon-supported metal electrocatalysts, metal particles appear as dark areas and low atomic weight carbon supports appear as light areas in the resultant micrographs due to differences in electron transmittance with increasing atomic weight [43, 44, 45-53]. The obtained information is often complemented by quantitative information such as total surface area and porosity.

Sample preparation

The TEM samples were prepared by suspending the supported Pt electrocatalysts powder in 90% ethanol solution followed by sonication of the suspensions for 10 minutes and depositing a drop of the suspension on a standard copper grid covered with carbon. Samples were mounted in a sample holder, which was introduced directly into the shaft of the microscope.

2.2.3 Scanning Electron Microscope (SEM)

Scanning electron microscopy (SEM) is a versatile imaging technique capable of producing three-dimensional images of material surfaces. SEM is one of the most frequently used instruments in material research today because of the combination of high magnification, large depth of focus, greater resolution and ease of sample observation [54]. SEM is used in this study to extract quantitative and qualitative information pertaining to agglomerate size/shape, particle morphology, and surface appearance of supported nanophase electrocatalysts.

A prerequisite for effective viewing is that the surface of the samples should be electrically conductive. During operation, electrons are deposited onto the sample. These electrons must be conducted away to earth thus conductive materials such as metals and carbon can be placed directly into the SEM whereas non-metallic samples have to be coated with a gold metal layer to be observed.

The basic operation in SEM entails the interaction of an accelerated highly monoenergetic electron beam, originating from a cathode filament, with the atoms at a sample surface. The electron beam is focused into a fine probe, which is rastered over the sample surface. The scattered electrons are collected by a detector, modulated, and amplified to produce an exact reconstruction of the sample surface and particle profile [55-60].

2.2.3.1 Energy dispersive spectroscopy

The elemental composition of the catalysts was investigated using energy dispersive spectroscopic (EDS) emission analysis which is coupled with a Hitachi X-650 SEM. Relative element concentrations were estimated using GENESIS software. Every sample was scanned five times to obtain the average wt.% of the metal. The operating parameters of the SEM are described in Table 2.4.

Table 2.4: Hitachi X-650 SEM operational parameters.

Parameter	**Setting**
Accelerating voltage	25keV
Tilt Angle	0°
Aperture	0.4mm
Resolution	3nm
Working distance	15mm

Specimen preparation

The conductive powders of the catalytic samples were dispersed upon the carbon stick tabs and mounted on an aluminum stub holder. After that, the holder was loaded into the spectrometer.

2.3 ELECTROCHEMICAL CHARACTERIZATION

Electrochemistry is a powerful and sensitive analytical tool used for both qualitative analysis and quantitative analysis of the catalyst activity.

Chronoamperometry was used in this study to screen the electrocatalysts in order to determine the electrochemical activity and stability of the Pt based binary catalysts.

Most of Amperometry is now a subclass of voltammetry in which the electrode is held at constant potentials for various lengths of time. Chronoamperometry is performed with a three-electrode cell. One of the three electrodes is the working electrode. The second electrode is a reference electrode, against which the potential of the working electrode is measured. The third electrode is called a counter electrode. This is necessary so that accurate measurement of the working electrode potential can be made.

In Chronoamperometry, the working electrode potential is suddenly stepped from an initial potential to a final potential, and the step usually crosses the formal potential of the analyte. The solution is not stirred. The initial potential is chosen so that no current flows (i.e., the electrode is held at a potential that neither oxidizes nor reduces the predominant form of the analyte). Then, the potential is stepped to a potential that either oxidizes or reduces the analyte, and a current begins to flow at the electrode. This current is quite large at first, but it rapidly decays as the analyte near the electrode is consumed, and a transient signal is observed.

2.3.1 Electrochemical activity investigation

The electrochemical investigation was performed with an **Autolab PGSTAT 30** (Eco Chemie BV, Netherlands) at room temperature. Connected to the Autolab was a flow rate control box which was used to control the flow of both the Hydrogen gas and Carbon monoxide gas purging through the electrode. The Hydrogen gas flow rate was kept at 50mL/min, throughout the experiment while the concentration of CO was increased from

0ppm-1000ppm, (10, 30, 50, 100, 300, 500 and 1000ppm). The 0.5M H_2SO_4 electrolyte solution was de-aerated with nitrogen for 1 hour prior to each analysis to eliminate the parasitic influence of oxygen on the analytical signal and to establish a baseline. The Gas diffusion electrode was then purged with H_2 gas only for 30 minutes to determine the Hydrogen Oxidation reaction. The experimental parameters are given in Table 2.5

Table 2.5 Experimental parameters for the electrochemical activity study.

Parameter	**Specification**
Electrolyte	0.5M H_2SO4
Working electrode	Gas diffusion electrode
Counter electrode	Platinum
Reference electrode	Ag/AgCl
Potential	0.35V
Time	900s

A thin film of ink, prepared as described below, was sprayed on a Gas diffusion electrode. Prior to spraying of the catalysts the carbon paper was measured to ensure that the correct area was achieved and weighed before and after spraying to determine the exact mass sprayed.

Catalyst ink preparation

Electrocatalyst inks were prepared by suspending 0.25mg catalyst powder in 500mg distilled water with the addition of 750mg of 5% alcoholic Nafion® solution. The ink was allowed to sonicate for 30 minutes. Then 5-10mL of iso-propanol was added and the suspension was ultrasonicated for a further one and a half hour. The ink was then sprayed to a gas diffusion electrode to obtain 0.25mg/cm^2 platinum loading. The membrane was pretreated as described in Section 2.1.4 and was pressed onto the electrode to obtain the

anode electrode assembly (AEA). The AEA is then assembled in a cell and subjected to electrochemical characterization.

CHAPTER 3

RESULTS AND DISCUSSION: STRUCTURAL CHARACTERIZATION OF NANOPHASE ELECTROCATALYSTS

In this chapter the results of the characterization and interpretation of platinum based binary catalysts will be presented. The investigation was initiated by a structural characterization study of different Pt based electrocatalysts. The electrochemical characterization of electrocatalysts and their comparison to the commercial standard Pt/C is presented in the following chapter. The electrochemical properties will be correlated with the structural study of electrocatalysts.

3.1 PHYSICO-CHEMICAL CHARACTERIZATION OF ELECTROCATALYSTS

3.1.1 Elemental composition study of Pt/C electrocatalyst

The elemental composition of the Pt based electrocatalysts was determined by EDS, following the procedure given in Section 2.2.3.1 The elemental composition study of commercial Pt based binary catalysts was conducted to compare the elemental state of the electrocatalysts before and after sintering in order to determine whether there is a significant change in the catalyst composition. The compositions of the catalysts sintered at various conditions are presented in Table 3.1. The results show that the sintering of catalysts does not have any significant effect on the elemental composition of the electrocatalysts.

Table 3.1 Elemental composition study obtained with EDS

Catalysts	Unsintered At. %	Sintered @ 350 At. %	Sintered @ 450 At. %
PtRu/C	1:1	1:1	1:1
PtSn/C	2.7:1	2.6:1	2.8:1
PtNi/C	1:1	1:1	1:1

3.1.2 Particle size and crystallinity study of Pt based electrocatalyst

The crystallinity of catalysts, particle size, degree of alloying and lattice spacing of Pt based electrocatalysts were determined using XRD, following the procedure given in Section 2.2.1. The corresponding patterns for each of the different electrocatalysts are shown in the following figures 3.1 to 3.4.

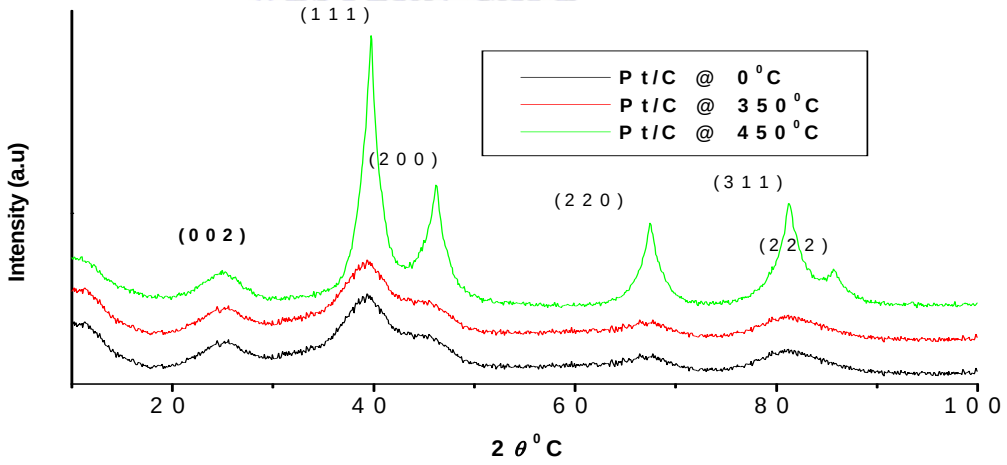

Fig. 3.1 *X-Ray diffraction patterns of Pt/C electrocatalyst sintered and unsintered.*

The broad diffraction peaks are observed in the diffractograms of the unsintered Pt/C and the sintered Pt/C at 350ºC. In both diffractograms, facets (200), (220) and (311) are broad and not clear, (222) is not visible at all and this is indicative of the small crystalline particle size.

The Pt (111) exhibited the highest intensity in the diffractograms suggesting high densities of (111) orientated crystals and (111) facet may be the most reactive in Pt/C. The XRD patterns of Pt/C sintered at 450 ºC show narrow and intense peaks, suggesting that the particles are more crystalline. All the catalysts exhibited an fcc structure with the intensity of the peaks increased with increasing sintering temperature, which is expected.

The particle size parameters, D and α (see the equations in Section 2.2.1), of Pt/C were calculated from the XRD spectra using the Pt (220) peak position and its width at half peak height. The results are listed in Table 3.2.

It can also be seen from Table 3.2 that the lattice parameters of the Pt (220) peak are around 3.9, showing that there is no change in the cubic crystalline Pt structure and that heat treatment had no effect on the physical morphology of the electrocatalyst as the particle size and the lattice spacing remained the same even when subjected under high temperatures.

Table 3.2: XRD analyses of unsintered and sintered commercial Pt/C

Sample	**D (nm)**	**α (Å)**	**$2\theta_{max}$ (degrees)**	**θ (degrees)**
20%Pt/C	3.1	3.93	67.6	33.8
20%Pt/C@ 350 ºC	3.1	3.93	67.6	33.8
20%Pt/C@ 450 ºC	3.1	3.93	67.6	33.8

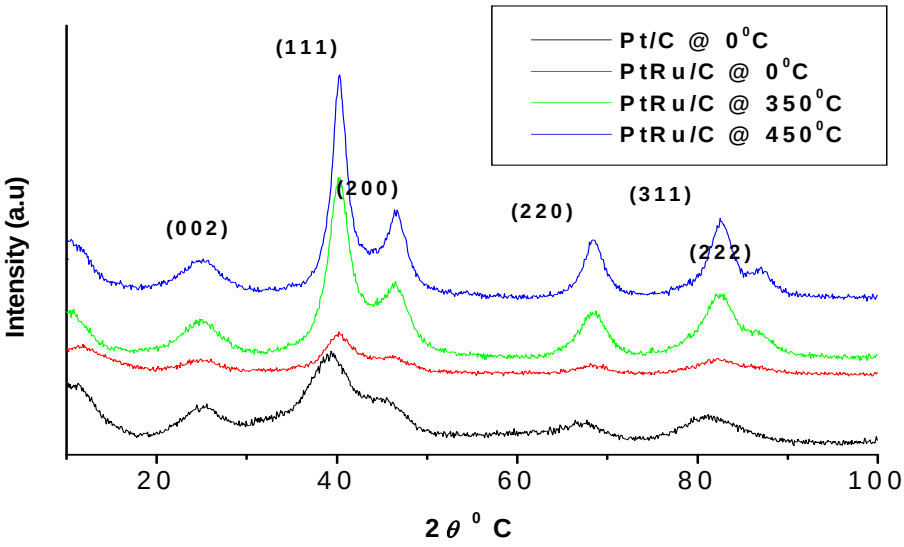

Fig. 3.2 *X-Ray diffraction patterns of PtRu/C electrocatalyst sintered and unsintered*

With the unsintered PtRu/C diffractogram, facets (200), (220) and (311) are broad and not clear, (222) is not visible at all. This just like with the Pt/C is indicative of the small crystalline particle size. However with the PtRu/C @ 350 ºC diffractogram, even though the peaks are still broad but they become more visible and distinct when compared to the former. This is when the face centered cubic structure of the PtRu/C is firstly observed.

Just like Pt/C the Pt (111) exhibited the highest intensity in the diffractograms suggesting high densities of (111) orientated crystals and that these may be the most reactive in both Pt/C and PtRu/C and it has been stated by Cattaneo et al. [61] that Pt (111) crystals have the lowest onset potential for methanol oxidation and the lowest CO_{ad}-poisoning rate in single crystal analysis. There is a clear shift of 2θ to higher angles when comparing with Pt/C and there is a change in width at half peak width.

The particle size **D** and the lattice parameter **α** were calculated from the Pt (220) peak position. For unsintered and sintered at 350 ºC and 450 ºC the particle size were 3.1nm, 3.2nm and 3.1nm respectively. The extremely small crystalline particle size of the

electrocatalysts maximizes the surface area exposed to the reactants allowing more reactions to occur thereby increasing the electrochemical activity of the catalyst. This relation of small particle size to enhanced activity can be confirmed from the electrochemical characterization results in Chapter 3.

Table 3.3: XRD analyses of sintered and unsintered commercial PtRu/C

Sample	**D (nm)**	**α (Å)**	**$2\theta_{max}$ (degrees)**	**θ (degrees)**
20%Pt/C	3.1	3.93	67.6	33.8
20%PtRu/C	3.2	3.90	68.1	34.1
20%PtRu/C@350 ºC	3.1	3.90	68.3	34.2
20%PtRu/C@ 450ºC	3.1	3.90	68.4	34.2

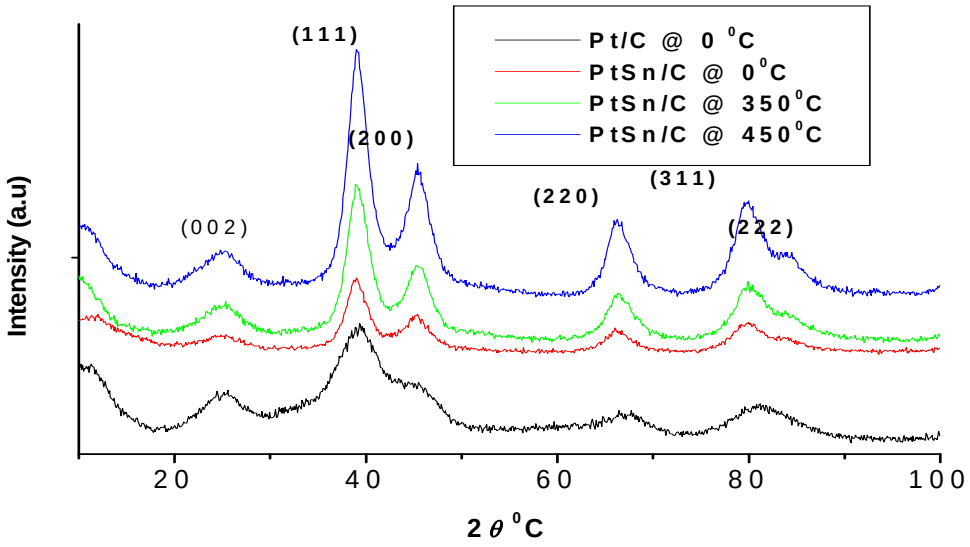

Fig. 3.3 *X-Ray diffraction patterns of PtSn/C electrocatalyst sintered and unsintered*

With PtSn/C the face centered cubic structure can be observed from the onset even though the facets (200), (220) and (311) are broad and with low intensity. (222) is also broad but unclear and can only be noticeable as the catalyst is sintered. It is because of the very small platinum particle sizes (which ranges from 2.9-300nm), that these peaks of these facets are broadened.

The relationship between crystalline particle size and the degree of alloying is observed in the D and the α (Å) values of PtSn/C. As it has been stated that the smaller the particle size the higher the electrochemical activity. If we take into consideration the particle size theory the activity of this catalyst observed from the results in Table 3.4 is (450 ºC>unsintered> 350 ºC) but in actual fact it is (450 ºC>350 ºC>unsintered) and this is confirmed by the Electrochemical results in chapter 4, because according to T. Frelink et. al [62-65] these bimetallic materials improve the catalytic effect of platinum by a bifunctional mechanism where partially oxidized M at the surface supplies oxygenated species for improving the oxidation of the adsorbates. A catalytic effect can also be explained by the ligand effect

where the metal M atoms close to Pt are expected to influence the density of electronic states of Pt, leading to the weakening of the Pt-CO bond.

Table 3.4: XRD analyses of sintered and unsintered commercial PtSn/C

Sample	**D (nm)**	**α (Å)**	**$2\theta_{max}$ (degrees)**	**θ (degrees)**
20%Pt/C	3.1	3.93	67.6	33.8
20%PtSn/C	2.9	3.90	66.0	33.0
20%PtSn/C@ 350ºC	3.0	3.90	66.5	33.3
20%PtSn/C@ 450ºC	3.0	3.90	66.5	33.3

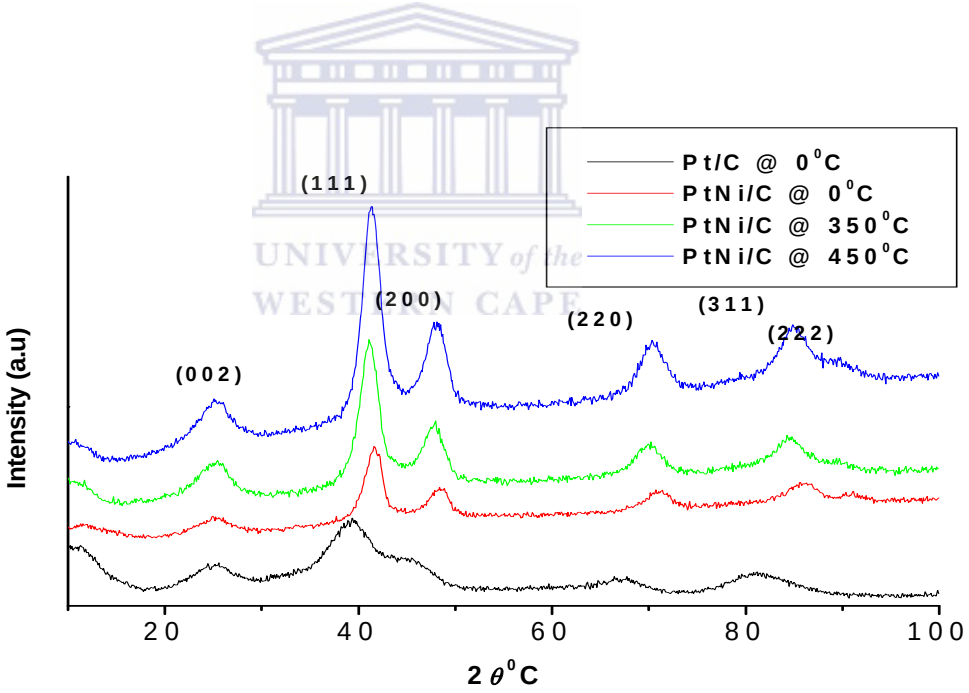

Fig. 3.4 *X-Ray diffraction patterns of PtNi/C electrocatalyst sintered and unsintered*

The visibility of facets in PtNi/C is almost similar to those observed in PtSn/C diffractograms. Also with PtNi/C it can be suggested that it exhibit a face centered cubic structure even though the Pt (222) facet is no clearly visible.

Particle size of the electrocatalyst between unsintered PtNi/C and sintered PtNi/C at 350ºC decrease as the electrocatalyst is sintered at higher temperatures thereby increasing the electrocatalytic activity. Between PtNi/C sintered at 350ºC and that sintered at 450ºC there is a noticeable difference in electrochemical activity (refer chapter 4), being the latter is more active than the former, this is due to the fact that Ni alloys retain much of their strength at elevated temperatures and are tough and ductile at low temperatures.

Table 3.5: XRD analyses of unsintered commercial PtNi/C

Sample	**D (nm)**	**α (Å)**	**$2\theta_{max}$ (degrees)**	**θ (degrees)**
20%Pt/C	3.1	3.93	67.6	33.8
20%PtNi/C	3.4	3.80	71.0	35.5
20%PtNi/C	3.3	3.80	70.1	35.0
20%PtNi/C	3.4	3.80	70.3	35.1

3.1.3 Particle size and particle size distribution of supported electrocatalysts

TEM was conducted to study the morphology of the electrocatalysts. It was used to determine the particle size and the particle size distribution of the electrocatalysts in order to support the XRD studies. The carbon support is visible in the TEM micrographs, as large grey particles with the small black Pt particles distributed upon them. Micrographs of TEM analysis for the Pt based electrocatalysts are presented in figure 3.5.

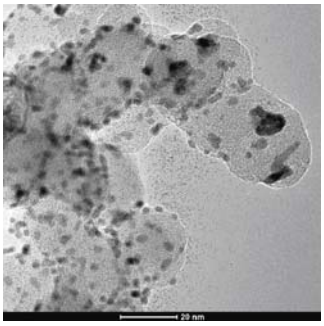

Fig 3.5a Unsintered Pt/C

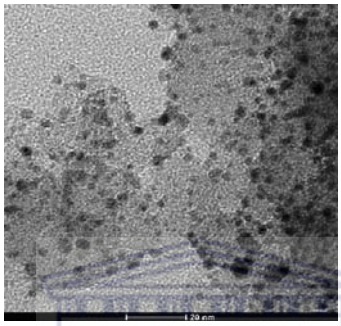

Fig 3.5b Pt/C sintered @350ºC

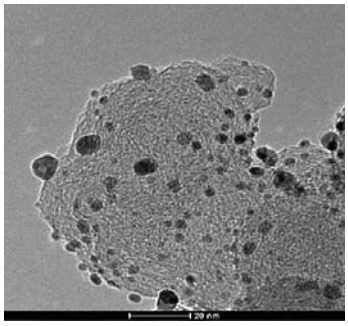

Fig 3.5c Pt/C sintered @450ºC

Pt nanoparticles in unsintered Pt/C micrograph are well dispersed on the carbon support. The Pt agglomerates are also observed on some parts of the sample. The Pt nanoparticles dispersed on the carbon support ranged from 2.4-3.5nm. The average particle size is 2.9nm. The TEM average particle size is in agreement with the particle size determined with the XRD which is 3.1nm.

The Pt/C sintered at 350ºC and 450ºC micrographs, show less agglomeration, high dispersion of the Pt nanoparticles on the support and easy identification of the Pt nanoparticles. The nanoparticle sizes of the Pt/C sintered at 350ºC and 450ºC ranges from 2.9-3.5nm and 2.4-2.9nm giving an average of 3.1nm and 2.6nm respectively

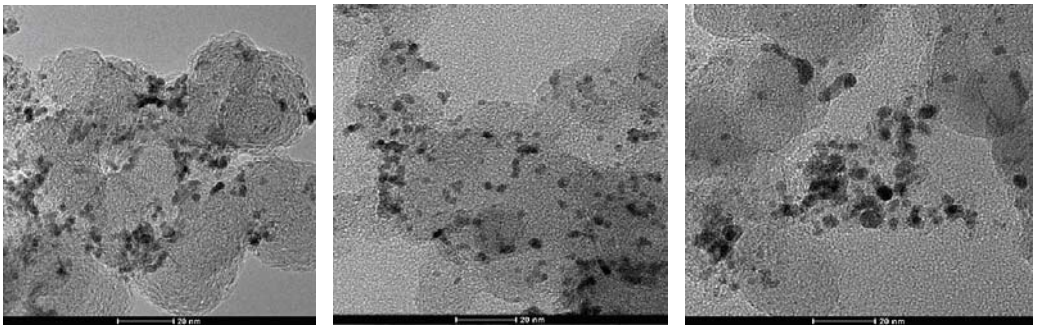

Fig. 3.6a Unsintered PtRu/C **Fig.3.6b** PtRu/C sintered @350ºC **Fig 3.6c** PtRu/C sintered @450ºC

Similar trends was noted for the PtRu/C catalysts (Figure 3.6), where the sintered catalysts at 350 ºC and 450 ºC showed the formation of agglomerates

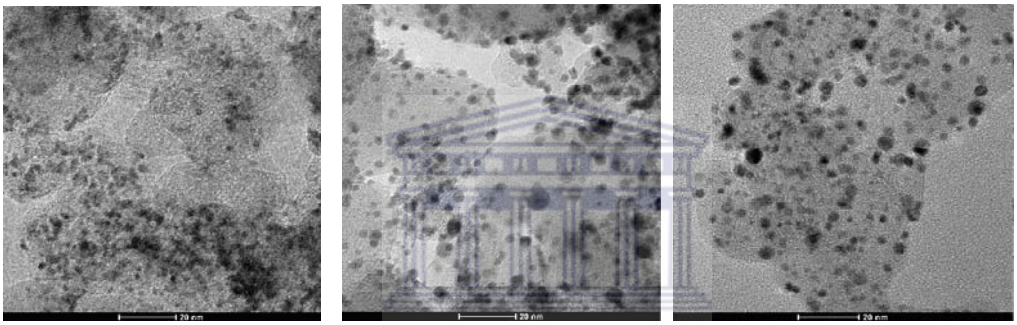

Fig 3.7a Unsintered PtSn/C **Fig.3.7b** PtSn/C sintered @350ºC **Fig 3.7c** PtSn/C sintered @450ºC

The TEM micrographs of PtSn/C catalysts are presented in Figure 3.7. No agglomeration of the particles was noted with the increase in sintering temperature as was noted for Pt/C and PtRu/C catalysts. The average nanoparticle size of the PtSn/C catalysts was found to be about 3.0nm.

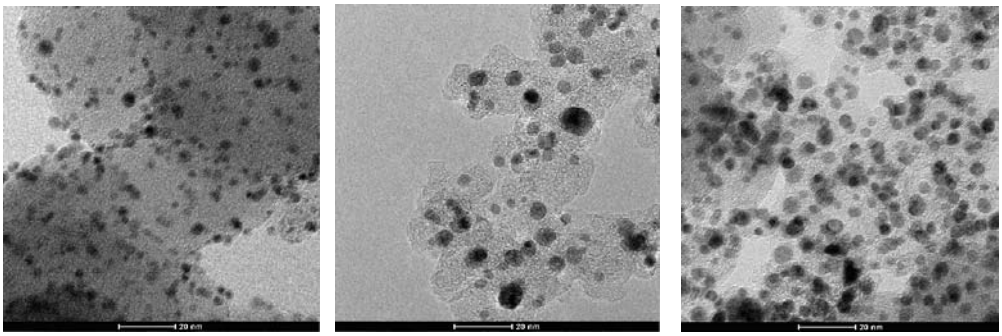

Fig 3.8a Unsintered PtNi/C **Fig.3.8b** PtNi/C sintered @350ºC **Fig 3.8c** PtNi/C sintered @450ºC

Fig. 3.8a is a micrograph of unsintered PtNi/C electrocatalyst. As compared to other unsintered catalysts, it shows the best particle dispersion and the particles are well defined and easier to identify. It is quite easy to distinguish between them and the support material. The nanoparticle size ranges from 2.9-3.5nm and the average size is 3.1nm.

But contrary to other sintered catalysts, one can note significant growth of particle size with sintering.

Chapter 4

RESULTS AND DISCUSSION: ELECTROCHEMICAL CHARACTERIZATION OF NANOPHASE ELECTROCATALYSTS

The physical characteristics of the catalysts were presented in Chapter *3*. The electrochemical characterization studying the activity of catalysts towards HOR and CO tolerance and their comparison to the commercial standard (BASF Pt/C) is presented and discussed in this chapter. The electrochemical properties subsequently characterized are correlated to the structural properties established in the previous chapter.

The electrochemical setup and characterization techniques were presented in Chapter 2. All the potentials measured and reported in this study are with respect to Ag/AgCl unless otherwise noted.

Presented below are the chronograms of the Pt based electrocatalysts. The screening of Pt based electrocatalysts was performed for both sintered and unsintered catalysts. Pt/C was used as a baseline for the binary electrocatalysts in order to compare their electrocatalytic activity. Chronoamperometric measurements of hydrogen oxidation current on the BASF Pt/C electrocatalyst electrode were carried out at 0.35 V (FC operating potential) for 900 s.

4.1 Platinum supported on carbon electrocatalyst (Pt/C)

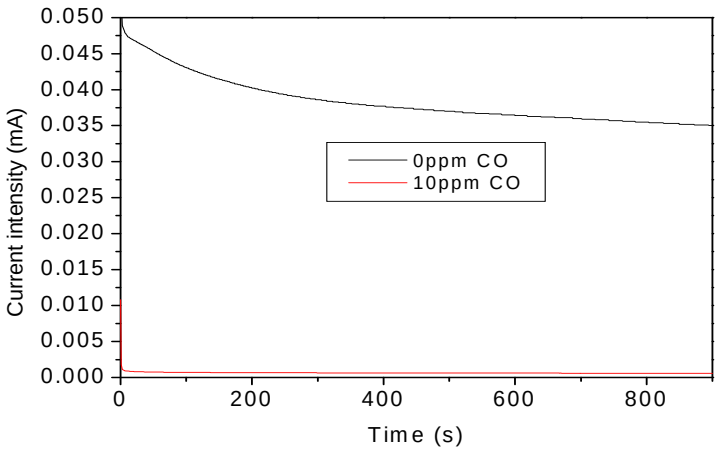

Fig.4.1 Unsintered Pt/C @ 0.35V (0ppm-10ppm CO)

Figure 4.1 shows the chronoamperometric graphs for Pt/C with pure hydrogen and with 10ppm CO. The activity of the catalyst is more than 50 times higher with pure hydrogen as compared with that of HOR with 10ppm CO. A noticeable decrease in the current of Pt/C is observed when the electrocatalyst is poisoned with only 10ppm CO from about 0.035 to 0.00062 mA. Therefore, as expected and reported extensively in the literature [66, 67], even at the lowest levels of CO poisoning (10ppm) the activity of Pt/C is lowered.

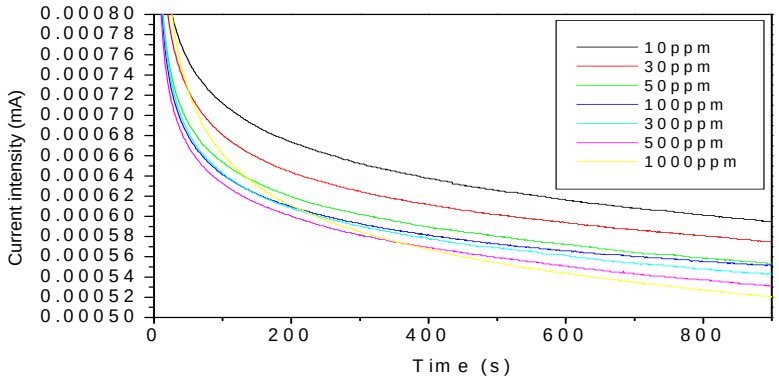

Fig.4.2 Unsintered Pt/C @ 0.35V (10ppm-1000ppm CO)

Figure 4.2 shows the HOR graphs with various concentrations of CO. When the concentration of CO is increased from 10ppm to 1000ppm the performance of Pt/C continues to deteriorate as expected but the decrease in the activity was not as significant as compared to that from 0ppm to 10ppm CO. This indicates that the surface of Pt/C catalyst is significantly covered with CO species at as low as 10ppm CO.

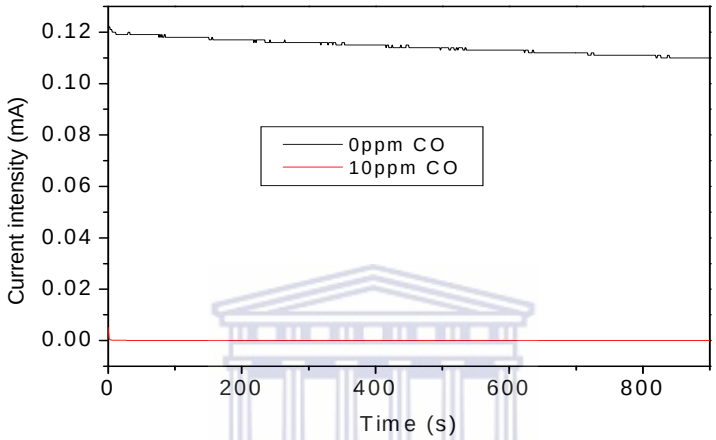

Fig.4.3 Sintered Pt/C @350ºC @ 0.35V (0ppm-10ppm CO)

Sintering at 350ºC favours the HOR in Pt/C (figure 4.3) as the current intensity increases from 0.035mA up to 0.1180 mA but the tolerance towards CO is lowered significantly from 0.00062mA to about 0.00021mA at 10ppm concentration, which is almost similar to that of unsintered catalyst. The results indicate that the activity of Pt/C catalysts towards HOR can be increased significantly by sintering the catalysts under controlled conditions but the CO tolerance can not be tailored through sintering.

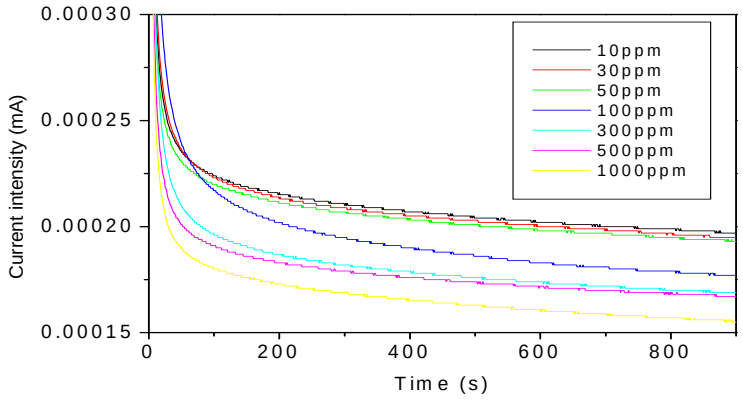

Fig.4.4 Sintered Pt/C @350ºC @ 0.35V (0ppm-1000ppm CO)

Figure 4.4 shows the HOR activity of the catalysts sintered at 350°C with various concentrations of CO. As the concentration of CO was increased the activity decreased.

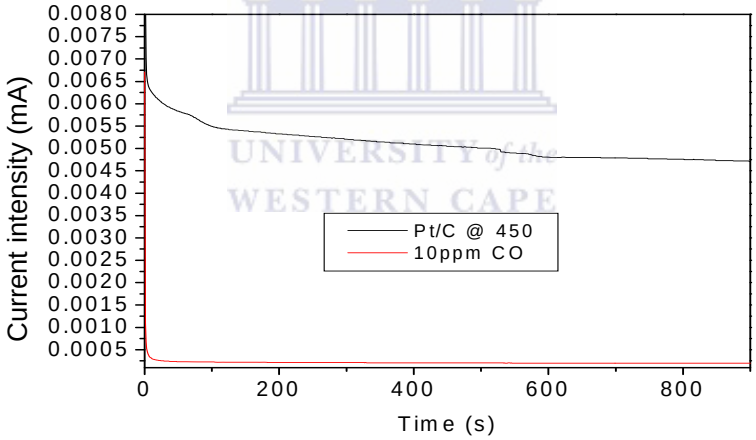

Fig.4.5 Sintered Pt/C @450ºC @ 0.35V (0ppm-10ppm CO)

The temperature was increased from 350 to 450°C and the activity is studied (Figure 4.5). The HOR activity of Pt/C was found to decrease at 450°C as compared to 350°C.

Therefore, it is evident that the electrochemical activity of Pt/C towards HOR is enhanced when the electrocatalysts is sintered at low temperatures but at high temperatures the activity of Pt/C drops towards the HOR and the tolerance towards the CO follow suit.

4.2 Platinum-Nickel supported on carbon electrocatalyst (PtNi/C)

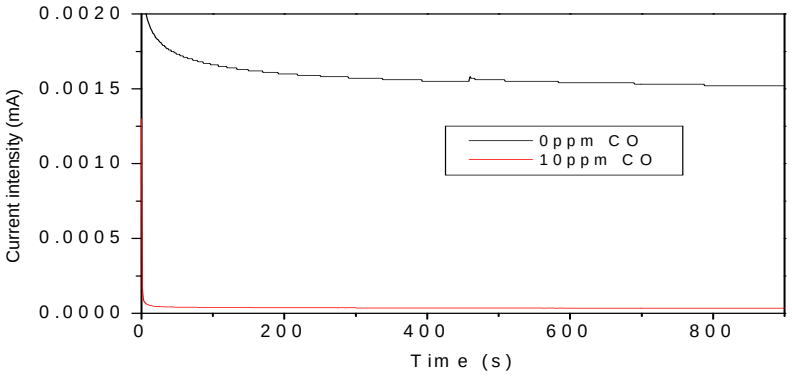

Fig.4.6 Unsintered PtNi/C @ 0.35V (0ppm-10ppm CO)

Figure 4.6 shows the graphs of unsintered PtNi/C catalyst representing their activity towards HOR. The activity of PtNi/C towards HOR is significantly lower as compared to Pt/C catalyst, which is expected since some of the active sites of Pt might have been masked by Ni molecules. The CO poisoning of PtNi/C catalysts was studied. The electrochemical activity of PtNi/C towards the HOR was 0.0015mA and then it decreased to 0.000034mA when it was poisoned with 10ppm CO. PtNi/C is expected to perform better than Pt/C since Ni is expected to impart electronic effects to Pt and thereby improving the CO tolerance as reported in the literature [68].

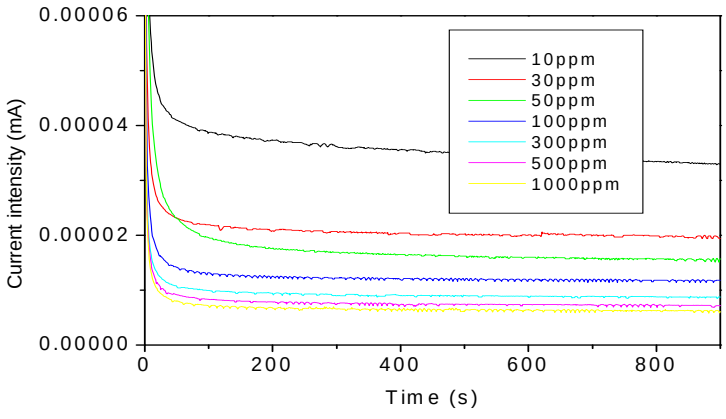

Fig.4.7 Unsintered PtNi/C @ 0.35V (0ppm-1000ppm CO)

As the concentration of CO was increased from 10ppm to 1000ppm (Figure 4.7) the current intensity decreased from about 0.000034 mA to about 0.000008 mA. A similar trend is noted for Pt/C catalysts.

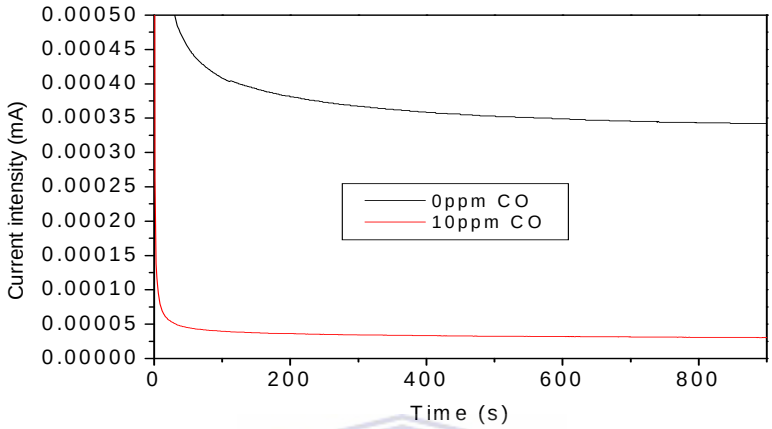

Fig.4.8 Sintered PtNi/C @350ºC @ 0.35V (0ppm-10ppm CO)

Fig.4.8, sintering the PtNi/C at 350ºC did not show any positive impact on its electrochemical activity. The electrochemical activity towards the HOR decreased from 0.0015mA to 0.00032mA. Also sintering PtNi/C catalysts did not improve the CO tolerance.

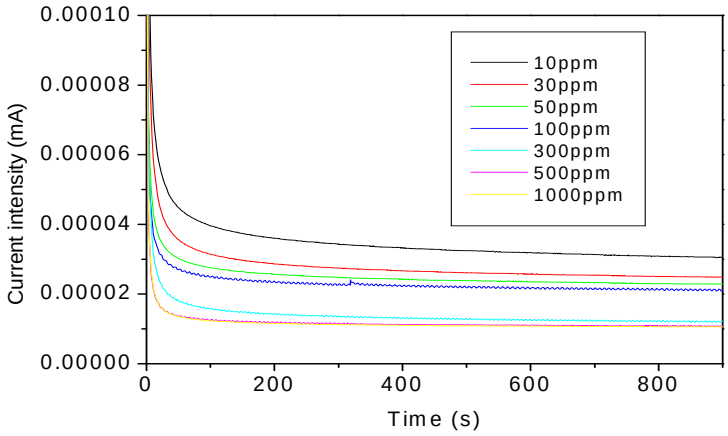

Fig.4.9 Sintered PtNi/C @350ºC @ 0.35V (0ppm-1000ppm CO)

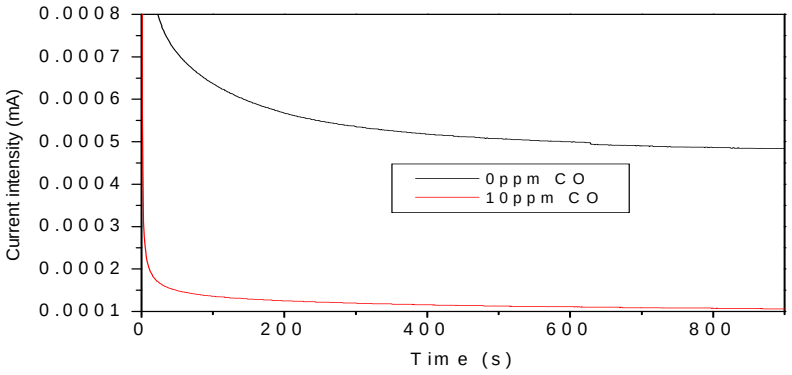

Fig.4.10 Sintered PtNi/C @450ºC @ 0.35V (0ppm-10ppm CO)

Although the activity of PtNi/C dropped at sintering at 350^{o}C, when sintered at 450^{o}C the activity was found to increase. This might be due to the higher dispersion of the catalysts at this sintering temperature. In spite of the increase, it was not good as Pt/C catalyst.

4.3 Platinum-Ruthenium supported on carbon electrocatalysts-PtRu/C

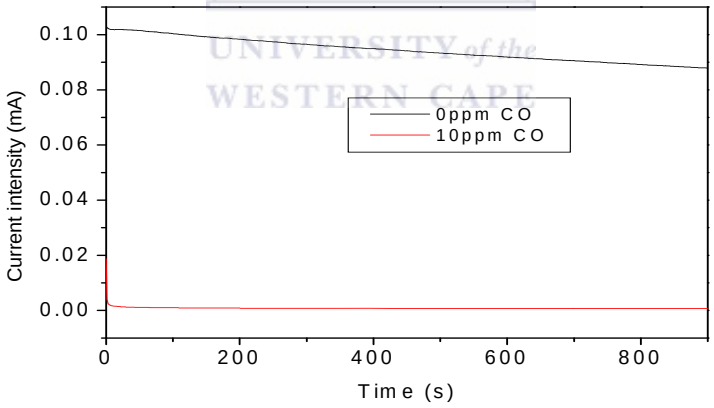

Fig.4.11 Unsintered PtRu/C @ 0.35V (0ppm-10ppm CO)

The activity of unsintered PtRu/C catalyst was found to be considerably higher than that of PtNi/C catalyst. The activity of PtRu/C catalyst drops considerably with 10ppm CO and was similar to that of Pt/C. The current intensity for PtRu/C when poisoned with 10ppm CO is 0.0016mA where as that of Pt/C and PtNi/C is 0.00062mA and 0.000037mA,

respectively. The HOR activity of PtRu/C catalyst is expected to be lower than that of Pt/C catalyst but with better CO tolerance.

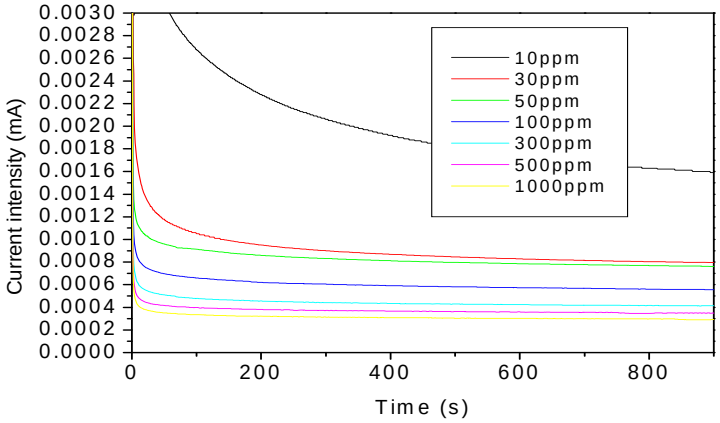

Fig.4.12 Unsintered PtRu/C @ 0.35V (0ppm-1000ppm CO)

Even though the electrochemical activity due to CO poisoning decreases the stability in PtRu/C continues even at higher ppm values. PtRu/C shows better tolerance towards the CO poisoning compared to PtNi/C and Pt/C.

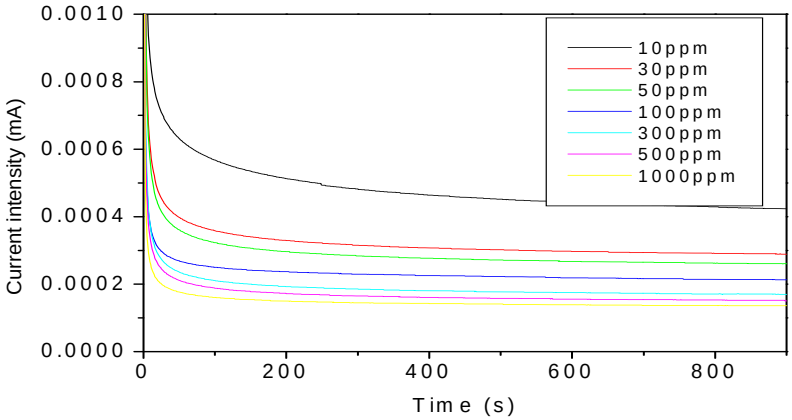

Fig.4.13 Sintered PtRu/C @350ºC @ 0.35V (0ppm-1000ppm CO)

As the ppm levels of CO increase the electrochemical activity of the electrocatalyst decrease but maintaining the stability.

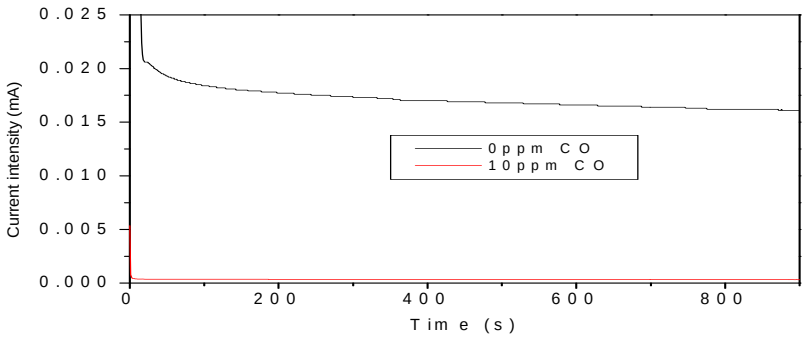

Fig 4.14 Sintered PtRu/C @450ºC @ 0.35V (0ppm-10ppm CO)

Sintering of PtRu at 450°C did not improve the activity of catalysts. The catalyst showed similar activity as that of 350°C sintered one. TEM studies, as discussed in chapter 3, did not show much difference in the size and distribution of PtRu catalysts at various sintering conditions. However, XRD results showed that the catalysts are better alloyed at higher sintering temperatures. The discrepancy in the electrochemical activity of PtRu catalyst as compared to reported ones needs to be investigated further with better insight into the surface compositions and oxidation states of the catalysts using XPS and EXAFS analysis.

4.4 Platinum-Tin supported on carbon-PtSn/C

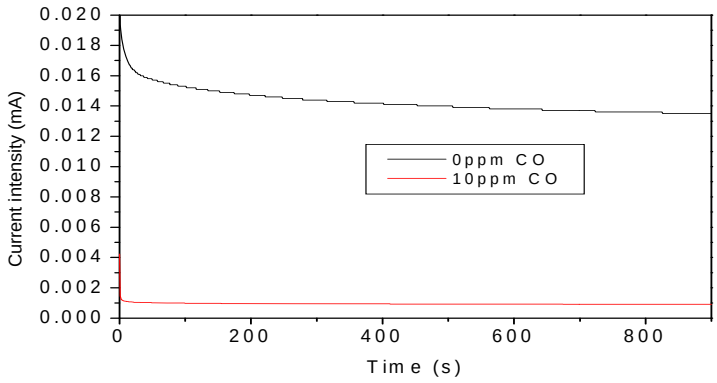

Fig.4.15 Unsintered PtSn/C @ 0.35V (0ppm-10ppm CO)

PtSn/C is not favoured for the HOR as compared to Pt/C as the current intensity for the HOR is about 0.035mA and 0.014mA for PtSn/C. But it showed a much better performance

towards the CO tolerance when compared to that of Pt/C whereby the current intensity is 0.00062mA and 0.00093 for PtSn/C.

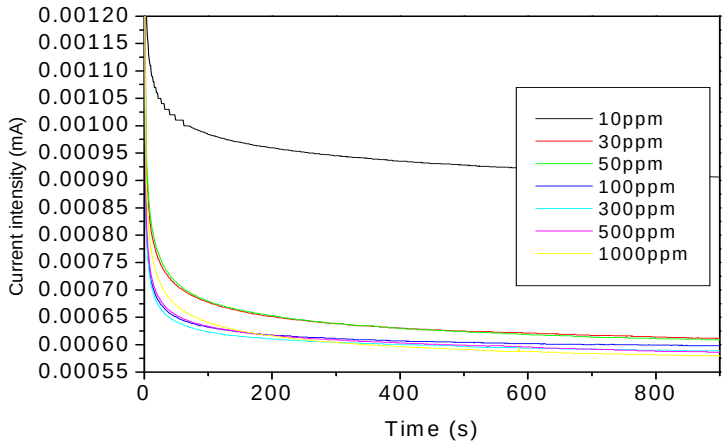

Fig.4.16 Unsintered PtSn/C @ 0.35V (0ppm-1000ppm CO)

The unsintered PtSn/C showed better tolerance for 10ppm CO and then there was a drop in current intensity but even though this is the case PtSn/C showed better tolerance to CO than Pt/C.

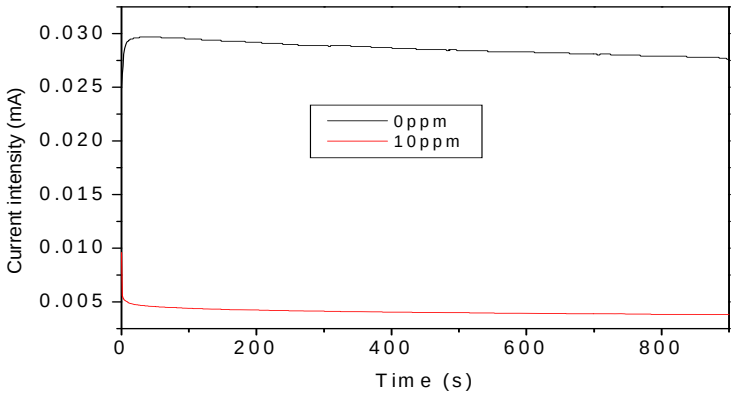

Fig 4.17 Sintered PtSn/C @350ºC @ 0.35V (0ppm-10ppm CO)

The sintering effect enhanced the electrochemical activity of PtSn/C towards the HOR; it is only for this electrocatalyst and Pt/C that this enhancement has been observed. With the other electrocatalysts the higher the temperature that the electrocatalyst is sintered at, the

lower the electrochemical activity towards the HOR. Also the electrochemical response to 10ppm CO poisoning is much better (0.00093mA to 0.00062mA of Pt/C).

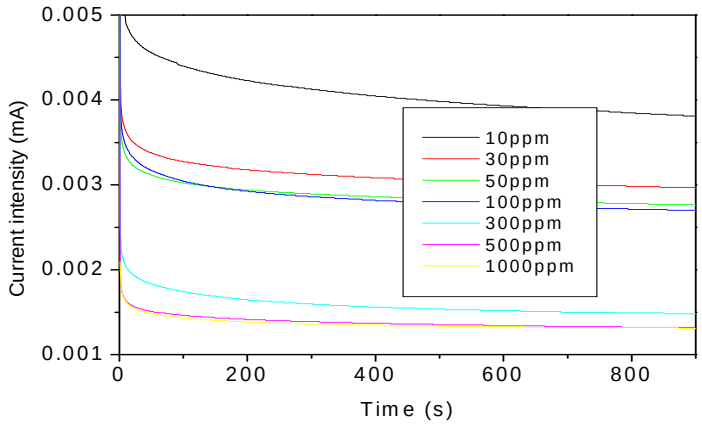

Fig 4.18 Sintered PtSn/C @350ºC @ 0.35V (10ppm-1000ppm CO)

The tolerance of PtSn/C towards the CO poisoning from 10ppm-1000ppm is much better than all the other electrocatalysts under study. Sintered PtSn/C was found to tolerate CO considerably better, over twice better than the best catalyst, even at concentrations up to 100ppm. Physical characterizations showed considerable alloying of PtSn catalysts with sintering and that the catalysts maintained better dispersion. This indicates that alloying of PtSn catalysts improved their activity towards HOR, especially the CO tolerance of PtSn.

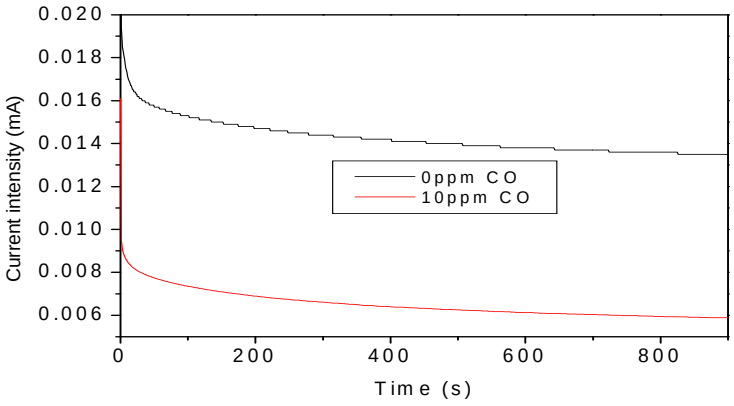

Fig 4.19 Sintered PtSn/C @450ºC @ 0.35V (0ppm-10ppm CO)

PtSn/C was sintered at 450°C and its activity and CO tolerance was studied. The electrochemical activity of the PtSn/C, sintered at 450ºC, towards the HOR decreased as compared to that sintered at 350°C but the tolerance towards 10ppm CO has improved. This indicates that increasing the alloying of PtSn catalysts will increase its CO tolerance.

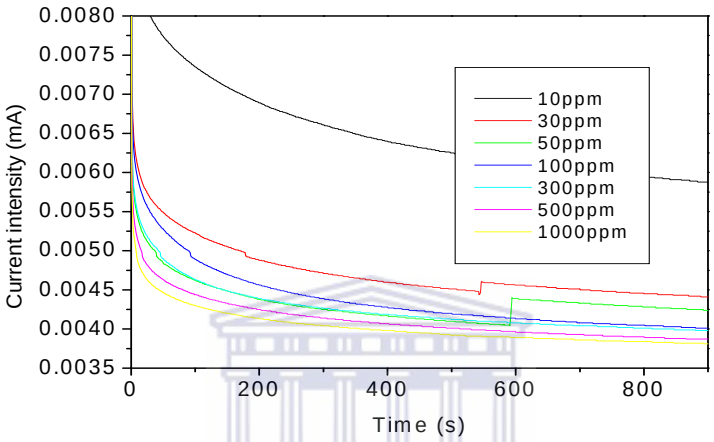

Fig 4.20 Sintered PtSn/C @450ºC @ 0.35V (10ppm-1000ppm CO)

The sintering of the electrocatalyst has enhanced the CO tolerance of PtSn/C. As it is observed from the above chromatogram the current intensity generated at 1000ppm CO poisoning is better than the current intensity generated at 10ppm CO poisoning for other electrocatalysts.

Chapter 5

CONCLUSIONS AND RECOMMENDATIONS

5.1 CONCLUSIONS

From the results presented in chapter 3 and 4, it can be concluded that sintering, which is also known as Heat Treatment, induces changes in catalysts properties such as particle size, morphology, dispersion of the metal on the support, alloying degree, electrocatalytic activity and electrocatalytic stability. It also plays a huge role on the catalyst surface morphology, all of which have a remarkable effect on Hydrogen Oxidation reaction (HOR). The results showed that the carbon surface composition, Pt nanoparticle size and Pt dispersion were significantly affected by the heat treatment.

Sintering induced changes in properties of the electrocatalysts such as the nanoparticle size, surface morphology, and dispersion of the metal on the support, alloying degree, electrocatalytic activity and stability.

As observed from the TEM monographs the surface morphology of the electrocatalysts changed from an amorphous to more ordered states. After sintering the Pt (111) facets exhibited the highest intensities suggesting high densities of Pt (111) orientated crystals which may be the most reactive in Pt/C and PtRu/C. TEM and XRD for both the heat treated and the untreated electrocatalysts showed that the electrocatalysts that are heat treated gave smaller particle size and a higher relative content of the Pt (111) crystal facets. XRD results showed that alloying of the catalysts increased with increased sintering temperature.

According to the SEM EDS results the electrocatalysts showed stability as their elemental composition remained unchanged after heat treatment.

Chronoamperometry was well suited to the electrochemical characterization of electrocatalysts due to its ability to readily identify highly active materials. Chronograms of Pt/C sintered at 350ºC showed a steady high current, suggesting stability and high electrochemical activity than when unsintered and when sintered at 450ºC.

Ni, as reported in the literature has good mechanical properties and excellent resistance to many corrosive environments. Therefore it is regarded as the best alloying element. Literature review of PtNi catalysts informed that PtNi retain much of their strength at elevated temperatures and are tough and ductile at low temperatures. The electrocatalytic activity and stability of PtNi/C is expected to better than that of Pt/C because PtNi/C is a binary electrocatalyst its electroactive surface area is larger and the combination of the bimetal properties is suppose to make it more electrocatalytic active however this has not been the case. However, the PtNi/C electrochemical results together with the XRD results are a confirmation of what other researchers have observed the fact that the decrease in particle size enhances the electrocatalyst behaviour. With the XRD the nanoparticle size of the unsintered PtNi/C was 3.30nm and when sintered at 350ºC and 450ºC the particle size slightly decreased from (3.40>3.30)nm respectively.

PtRu/C catalysts were studied with respect to their CO tolerance and HOR activity. According to [30, 31] reducing the particle size may not always work due to structure sensitive behaviour whereby the activity tends to deviate from that of the bulk. This is true when we look at the activity pattern of PtRu/C because with XRD the particle size decreased as the sintering temperature was increased however this decrease did not favour the CO tolerance because the chronogram of PtRu/C sintered @ 350ºC shows a decrease in electrochemical activity when compared to the chronogram of unsintered PtRu/C.

In the chronograms of PtSn/C, as the sintering temperature increases, so is the tolerance of CO poisoning. With the XRD results the nanoparticle size was observed as follows 2.9nm when unsintered, 3.00nm when sintered at 350ºC and 2.9nm when sintered at 450ºC. These bimetallic materials improved the catalytic effect of platinum by a bifunctional mechanism where partially oxidized M at the surface supplies oxygenated species for improving the oxidation of the adsorbates. A catalytic effect can also be explained by the ligand effect where the metal M atoms close to Pt are expected to influence the density of electronic states of Pt, leading to the weakening of the Pt-CO bond [62-65].

The best of all the electrocatalysts

The best of all the electrocatalysts at four concentrations of CO (0ppm, 10ppm, 100ppm and 1000ppm) were plotted against each other to compare their electrochemical activity and is presented in Figures 5.1 to 5.4 below. As observed from the chromatograms, the electrocatalyst that favors the HOR the most is Pt/C when pure hydrogen was used as the reactant.

However, the main aim of this study is to identify a Pt based electrocatalyst that best tolerates the CO poisoning so that it can be employed as anode electrocatalyst for PEMFC applications where reformed hydrogen is used as the fuel. Hence in that regard starting from 10ppm concentration of CO poisoning to 1000ppm, PtSn/C showed the best CO tolerance.

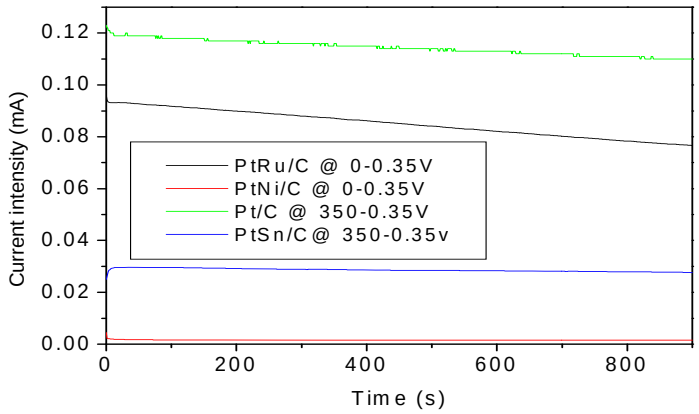

Fig 5.1 Best of the electrocatalysts @ 0.35V (0ppm CO)

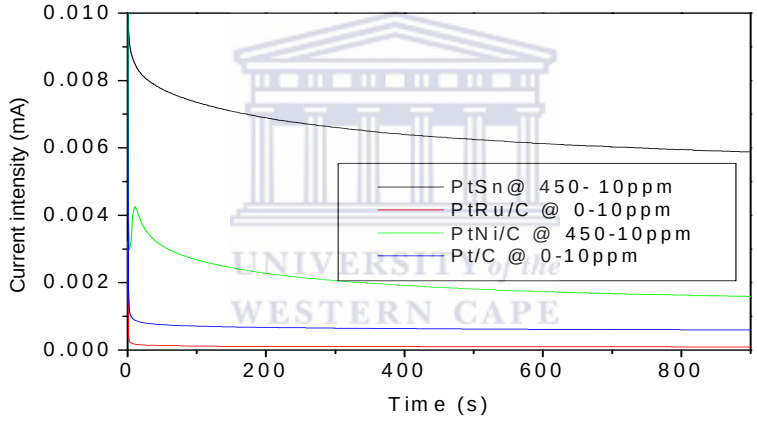

Fig 5.2 Best of the electrocatalysts @ 0.35V (10ppm CO)

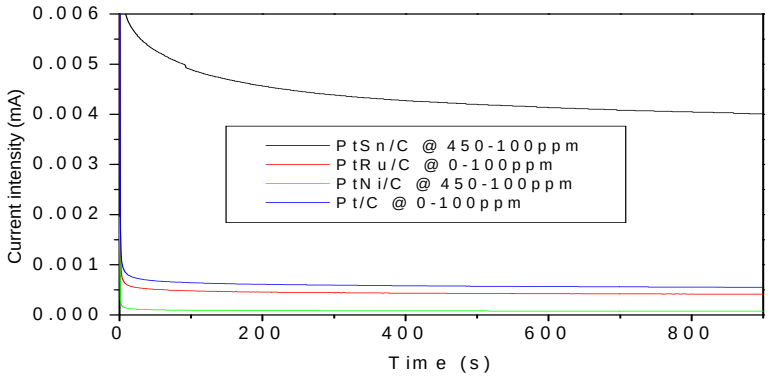

Fig 5.3 Best of the electrocatalysts @ 0.35V (100ppm CO)

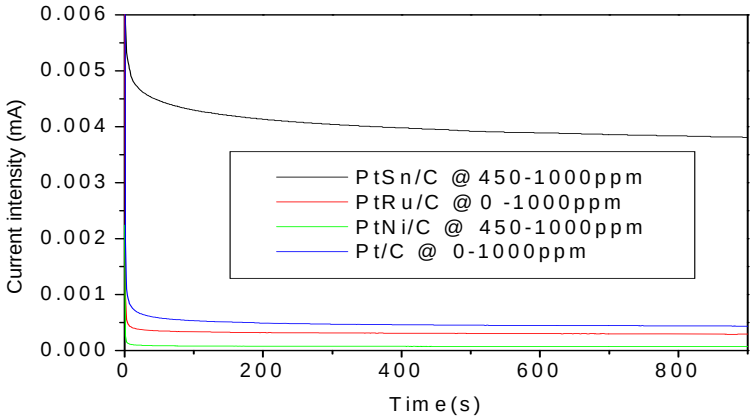

Fig 5.4 Best of the electrocatalysts @ 0.35V (1000ppm CO)

5.2 RECOMMENDATIONS

Platinum based binary catalysts were studied for their HOR activity and CO tolerance with a help of a three-electrode cell. PtSn catalyst was found to have the highest CO tolerance. The main recommendation from this study is to employ PtSn/C catalysts as the anode electrode and evaluate its performance in an MEA under PEMFC operating conditions. It is expected that PtSn catalyst might perform significantly better than Pt/C and PtRu/C catalysts, especially with CO impurities. Another recommendation is to employ other physical characterization techniques such as XPS and EXAFS in order to gain further insight into their activity and behaviour so that better catalysts with high CO tolerance can be designed.

REFERENCES

[1] *Timeline of hydrogen technologies*, [Online], Available: 04 February, (2009) http://en.wikipedia.org/wiki/Fuel_cell

[2] Types of fuel cells, [Online], Available: 04 February, (2009), http://www.rmi.org/sitepages/pid201.php

[3] Proton exchange membrane fuel cell, [Online], Available: 01 November, (2008), http://en.wikipedia.org/wiki/Fuel_cell

[4] Heterogeneous Catalysis, [Online], Available: 04 February, (2009), http://en.wikipedia.org/wiki/Heterogeneous_catalysis

[5] Homogeneous Catalysis, [Online], Available: 04 February, (2009), http://en.wikipedia.org/wiki/Homogeneous_catalysis

[6] W.Z. Li, "The research of cathode carbon support platinum catalyst for direct methanol fuel cell", Published PhD. thesis, Dalian Institute of Chemical Physics, (2003)

[7] G. Hoogers, "Fuel Cell Technology Handbook" by CRC Press LLC, (2003)

[8] W. Vielstich, A. Lamm, H. Gasteiger, "Handbook of Fuel Cells, Fundamentals Technology and Applications", volume1 , Printed and bound in Great Britain by Antony Rowe, Chippenham, Wiltshire, August (2005) p. 314

[9] H. Bönnemann, *J. Power Sources*, (1994), 84, 161

[10] H. Bönnemann, W. Brijoux in "Advanced Catalysis and Nano-structured Materials", Ed., W. Moser, Academic Press, (1996), p. 165

[11] T.J. Schmidt, et al. *J. Electrochem. Soc*., (1998), 145, 925

[12] R. Adams, R.J. Shriner, *J. Am. Chem. Soc.,* (1923), 45, 2171

[13] SR. Wang, P.S Fedkiw *J Electrochem Soc,* (1992) 139:3151

[14] K. Kinoshita, "Carbon, Electrochemical and Physicochemical Properties", John Wiley & Sons, New York, USA, (1988), p. 76.

[15] Y.S Kang Bae, C.H Lee., "Carbon" 43 (2005) p.1512–1516

[16] N Mazurek, C Benker, H Roth, Fuess, *Fuel Cells 6* (2006) 208– 213.

[17] H. Cheng, W. Yan, K. Scott, *Fuel Cells 7* (2007) 16–20

[18] K.S. Han, Y.S. Moon, O.H. Han, K.J. Hwang, I. Kim, H. Kim, *Electrochem Commun. 9* (2007) 317–32415.

(a) S.-W. Kim, M. Kim; W. Y Lee, T. J Hyeon, *Am. Chem. Soc.* (2002), 124, 7642.

(b) H. P Liang; H. M. Zhang; J.S. Hu; Y. G. Guo,; L. J. Wan,; C. L. Bai, Angew. *Chem., Int. Ed.* (2004), 43, 1540.

[19] (a) M. V Brussel, G. Kokkinidis,.; I. Vandendael; C Buess-Herman,. *Electrochem.Commun*. (2002), 4, 808.

(b) C. Coutanceau, M. J. Croissant, T.Napporn, C. Lamy, *Electrochim. Acta* (2000), 46, 579.

(c) M. C Gutierrez, M. J. Hortiguela, J. M. Amarilla, R Jimenez, M. L. Ferrer, F. J del Monte, *Phys. Chem . C* (2007), 111, 5557.

(d) A. Kongkanand, K. Vinodgopal, S. Kuwabata, P. V. J. Kamat, *Phys. Chem. B* (2006), 110, 16185.

(e) Y Mu, H Liang, J Hu, L Jiang, L. J Wan, *Phys. Chem. B* (2005), 109, 22212.

[20] (a) N. M. Markovic, T. J. Schmidt; V. Stamenkovic; P. N. Ross, "Fuel Cells" (2001),1, 105.

(b) M.-H. Shao; K. Sasaki; R. R. J. Adzic, *Am. Chem. Soc*. (2006), 128, 3526.

(c) S. J. Kim; C. S. Ah; D. J. Jang, AdV. Mater. (2007), 19, 1064.

(d) G. Chen; D. Xia; Z. Nie; Z. Wang; W. L Ang; L. Zhang.; J. Zhang, *Chem. Mater*. (2007), 19, 1840.

[21] L. Zhang, J. Zhang, D.P. Wilkson, H. Wang, J. *Power Sources* **156** (2006) 171,182.

[22] R. Bashyam, P. Zelenay, "Nature" **443** (2006) 63–66.

[23] B. Wang, *J. Power Sources* **152** (2005) 1–15.

[24] K.S. Han, Y.S. Moon, O.H. Han, K.J. Hwang, I. Kim, H. Kim, *Electrochem. Commun.* **9** (2007) 317–324.

[25] P. Vasudevan, Santosh, M. Neelam, S. Tyagi, "Transition Met. Chem." **15** (1990) 81–90.

[26] J. Luo, N. Kariuki, L. Han, L. Wang, C.J. Zhong, T. He, *Electrochim. Acta* **51** (2006) 4821–4827.

[27] P.L. Antonucci, V. Alderucci, N. Giordano, D.L. Cocke, H. Kim, *J. Appl. Electrochem*. **24** (1994) 58–65.

[28] S.J. Mukerjee, *App. Electrochem.* **20** (1990) 537–548.

[29] A. Elzing, A. van Der Putten, W. Visscher, E. Barendrecht, *J. Electroanal. Chem.* **200** (1986) 313–322.

[30] F. Coloma, A.S. Escribano, J.L.G. Fierro, F. Rodr´iguez-Reinoso, *Langmuir* **10** (1994) 750–755

[31] U. Bossel, "The Birth of the Fuel Cell" 1835 - 1845, 1st ed., European Fuel Cell Forum, Oberrohrdorf, Switzerland (2000)

[32] S.J. Mukerjee, *App. Electrochem. 20* (1990) 537–548

[33] R. Iannielo, VM .Schmidt, U. Stimming, J Stumper, A. Wallau, *Electrochim Acta* **39** (1994) 1863

[34] H.A. Gasteiger, N. Markovic, P.N. Ross, E.J. Cairns *J Phys Chem. **98*** (1994) 617

[35] S.R Wang., P.S. Fedkiw, *J Electrochem Soc* **139** (1992) 3151

[36] S.J. Lee, S. Mukerjee, E.A Ticianelli, J. McBreen, *Electrochim Acta* **44** (1999) 3283

[37] M. Watanabe, S. Motoo, *Electroanal Chem. Interfacial Electrochem* **60** (1975) 267

[38] B. Beden, C. Lamy, N.R. Tacconi, C. Arvia, *Electrochim Acta* **35** (1990) 691

[39] Y. Morimoto, E. Yeager, *J. Electroanal. Chem*. **441**, (1998) 77-81

[40] H. Hoster, T. Iwasita, H. Baumgartner, W. Vielstich, *J. Electrochem. Soc*., **148** (5) (2001) A496

[41] "Crystallite Size and Microstrain Analysis of Thin Films", (2005), [Online], Available: http://www.rigakumsc.com/contract/amia_res_TN-C01.htm

[42] J.M. Xu, X.B. Zhang, Y. Li, X.Y. Tao, F. Chen, T. Li, Y. Bao, H.J. Geise, *Diamond & Related Materials* **13** (2004) 1807– 1811

[43] G.C. Bond, *Chem. Soc. Rev*. **20** (1991) 441

[44] S. Mukerjee; In-Situ X-ray Absorption Spectroscopy of Carbon-Supported Pt and Pt-Alloy Electrocatalytic Activity with Particle Size and Alloying, *Catalysis and Electrocatalysis at Nanoparticle Surfaces*, New York, Marcel Dekker Inc. **14;** (2003) 501-530.

[45] B Fultz, J.M Howe; "Transmission Electron Microscopy and Diffractometry of Materials" 2nd Edition, Berlin, Springer-Verlag, **2** (2002) 63, **4**:203-213, 7:339

[46] S.C. Tsang, P.de Oliveira., J.J Davis, M.L.H Green., H.A.O Hill. *Chemical Physics Letters;* **249** (1996) 413-422

[47] M.M.J Treacy; Detection and Imaging of Supported Catalyst Particles, *Materials Problem Solving with the Transmission Electron Microscope*, Hobbs. L. W. Westmacott. K.H, Williams. D.B. (editors), Pittsburgh, Materials Research Society, **62** (1986) 367-378

[48] P. Ganesan., H.K Kuo, A Saavedra; R.J De Angelis. *Journal of Catalysis*, **52** (1978) 310-320.

[49] G.L Hornyak, S.T Peschel, T.H Sawitowski, G. Schmid. *Micron*, **29** (1998) 183-190

[50] P.S. Sklad.;The Preparation of TEM Specimens form Hazardous or Difficult Materials, *Specimen Preparation for Transmission Electron Microscopy of Materials*, Bravman. J.C, Anderson, R.M. Macdonald. M.L. (editors), Pittsburgh, Materials Research Society, **115** (1988) 39-50

[51] S.B. Rice, M.J. Treacy; The Art of the Possible: *An Overview of Catalyst Specimen Preparation Techniques for TEM Studies*, Bravman. J.C. Anderson. R.M. McDonald. M.L. (ed.), Specimen Preparation for Transmission Electron Microscopy of Materials, Pittsburgh, Materials Research Society, **115** (1988) 15-27

[52] K Han, K. Yu-Zhang; *Scripta Materialia*, **50** (2004) 781-786.

[53] K.J. Chao, C.N. Wu, A.S Chang, S.F.Hu. *Microporous and Mesoporous Materials*, **27** (1999): 287-295

[54] O.V. Cherstiouk, P.A Simonov, B.R. Savinova, *Electrochimica Acta* **48** (2003) 3851-3860

[56] H.R.J.R Van Helleputte, T.B.J Haddeman, M.J Verheijen., J.-J Baalbergen Microelectronic Engineering, **27**. (1995) 547-550.

[57] T.E Müller, D.G. Reid, W.K Hsu, J.P Hare, H.W. Kroto, D.R.M Walton. *Carbon*, **35** (1997) 495-502.

[58] J.I. Goldstein, D.E Newbury, P Echlin, D.C Joy, C Fiori., E. Lifshin..Scanning Electron Microscopy and X-ray Microanalysis: A Text for Biologists, Materials Scientists, and Geologists, New York, Plenum Press, **1**(1981) 1-3, **6**:275-278.

[59] C.W. Oatley; The Scanning Electron Microscope, Part 1: the Instrument, London, Cambridge University Press, **1**(1972) 1-2.

[60] D.E. Newbury, D.C Joy, P Echlin, C.E Fiori, J.I. Goldstein. *Advanced* Scanning Electron Microscopy and X-ray Microanalysis, New York, Plenum Press, (1986) **5**:186, **7**:295

[61] C. Cattaneo, Sanchez de Pinto. M.I, Mishima. H, Lòpez de Mishima. B.A, Lescano. D, Cornaglia. L. Journal of Electroanalytical Chemistry **461**(1999) 32-39.

[62] T. Frelink; W. Vissche; J.A.R. Van Veen; *Langmuir* **1996**, *12*, 3702.

[63] C. Lu; C. Rice; M. Masel; P.K. Babu; P. Waszczuk; H.S. Kim; E. Oldfield;A. Wieckowski; *J. Phys. Chem. B* **2002**, *106*, 958.

[64] R. Liu; H. Iddir; Q. Fan; G. Hou; A. Bo; K. L Ley; E.S.Smotkin; Y-E.Sung; H. Kim; S. Thomas; A. Wieckowski; *J. Phys. Chem. B* **2000**, *104*, 3518.

[65] J. P. I. Souza; F. J. B. Rabelo; I. R. de Moraes; F. C Nart; *J.Electroanal.Chem.* (**1997)** *420*, 17.

[66] H. F. Oetjen, V. M. Schmidt, U. Stimming, and F. Trila, J. Electrochem. Soc., (1996) 143, 3838.

[67] J. Divisek, H. F. Oetjen, V. Peinecke, V. M. Schmidt and U. Stimming, Electrochimica Acta, (1998) 43, 3811

[68] A.Wokaun, Ed. “Erneuerbare Energien“, 1st ed, B.G. Teubner, Stuttgart (1999)